



New Approaches to the Crystal Collimation

Victor Tikhomirov

Institute for Nuclear Problems Minsk, Republic of Belarus

UA9 Workshop, Roma, 23-25 February 2011

Outline

Beam collimation by crystals

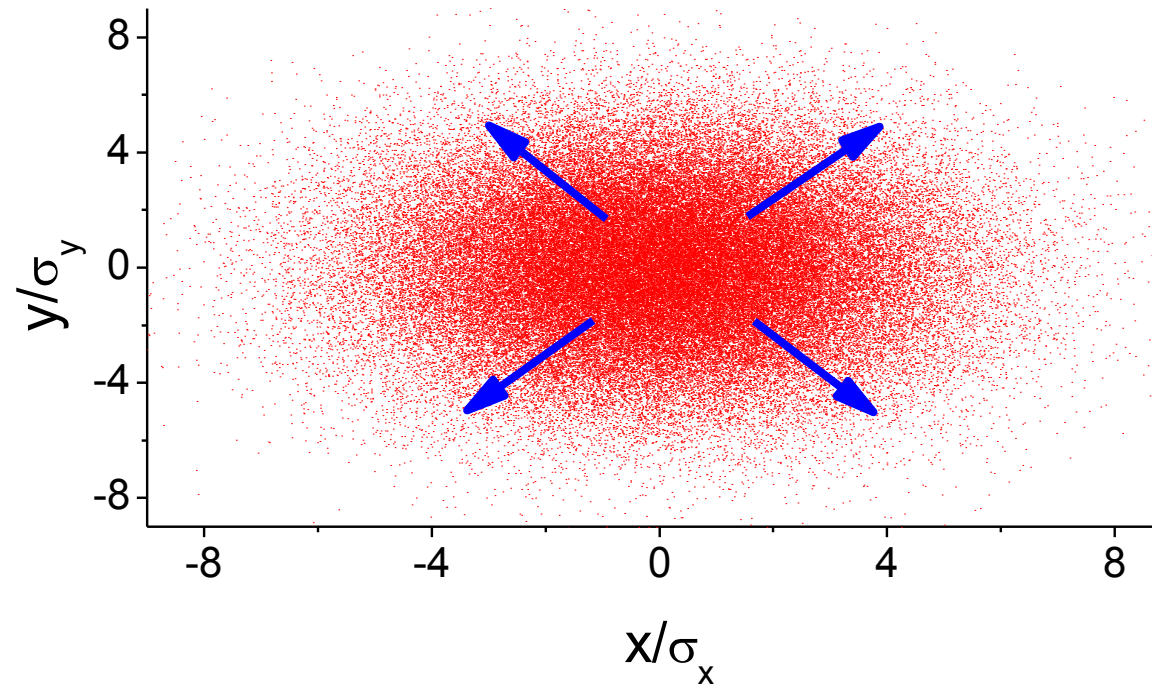
MVROC – Multiple Volume Reflection in One crystal (VR amplification by crystal axes)

Channeling fraction increase by the **crystal cut**

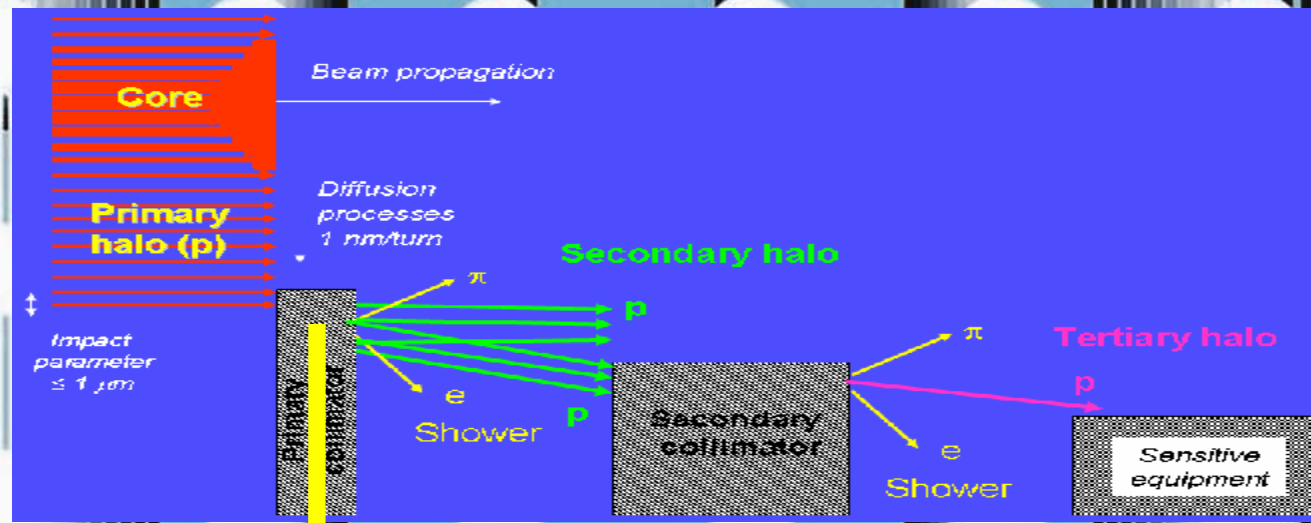
Crystal cut and MVROC **application to crystal collimation**

Conclusions

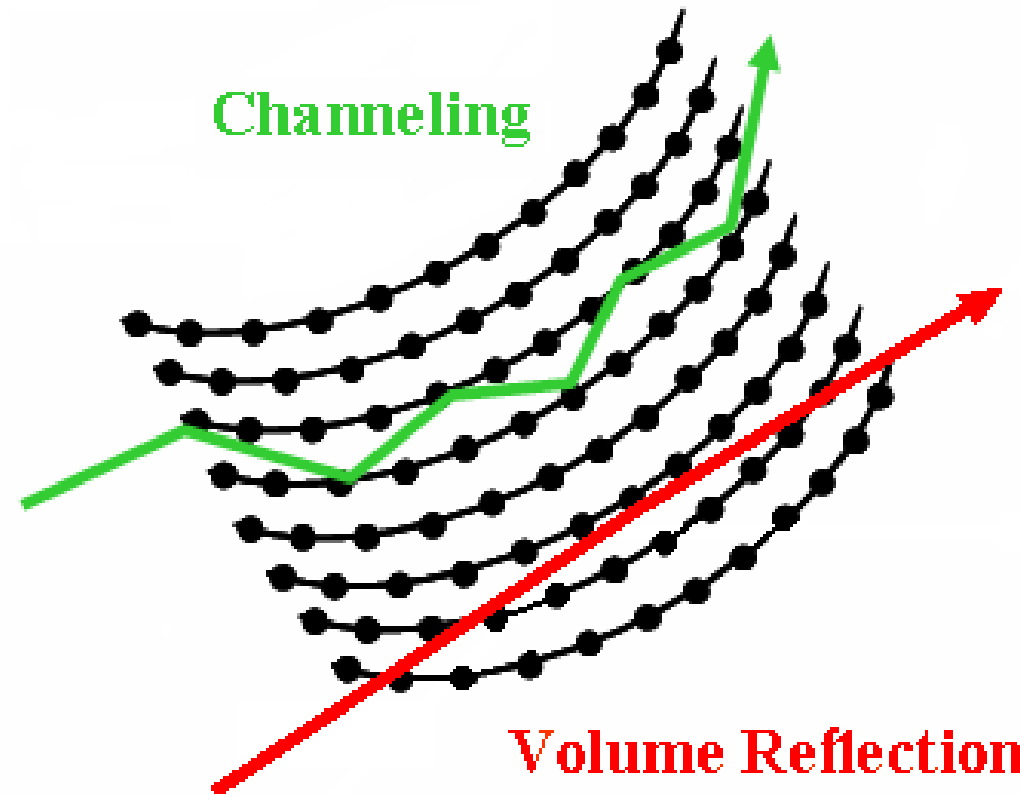
The planned LHC luminosity upgrade will intensify the beam **halo** formation



Crystals improve collimation efficiency



Crystals are used in either *channeling*
or volume reflection regimes



First results on the SPS beam collimation with bent crystals

W. Scandale et al, PLB 692(2010)78

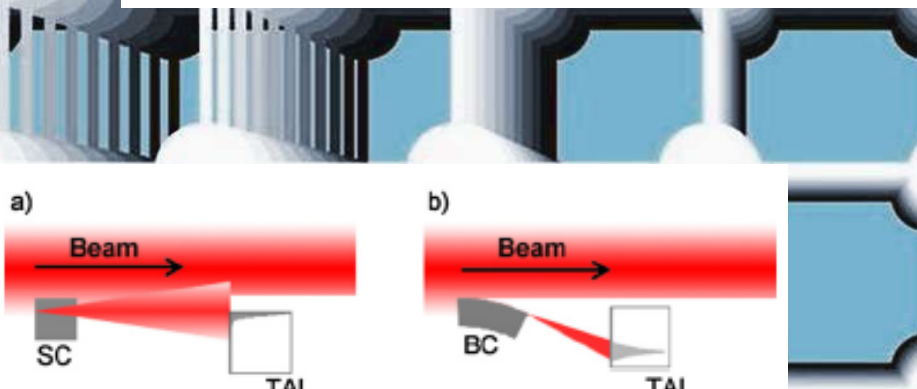


Fig. 1. (Color online.) (a) Collimation scheme using a solid state primary collimator-scatterer (SC). (b) Collimation scheme with a bent crystal (BC) as a primary collimator. Halo particles are deflected and directed onto the absorber (TAL - Target Aperture Limitation) far from its edge.

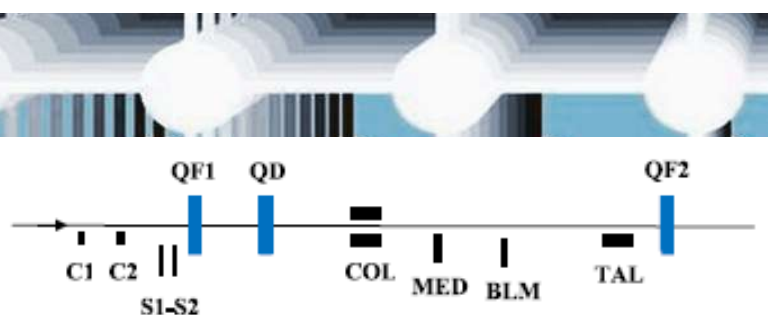


Fig. 2. (Color online.) The UA9 experimental layout. The primary collimators – bent crystals C1 and C2 are located upstream the quadrupole QF518 (QF1). The TAL acting as a secondary collimator (absorber) is upstream the quadrupole QF 520 (QF2).

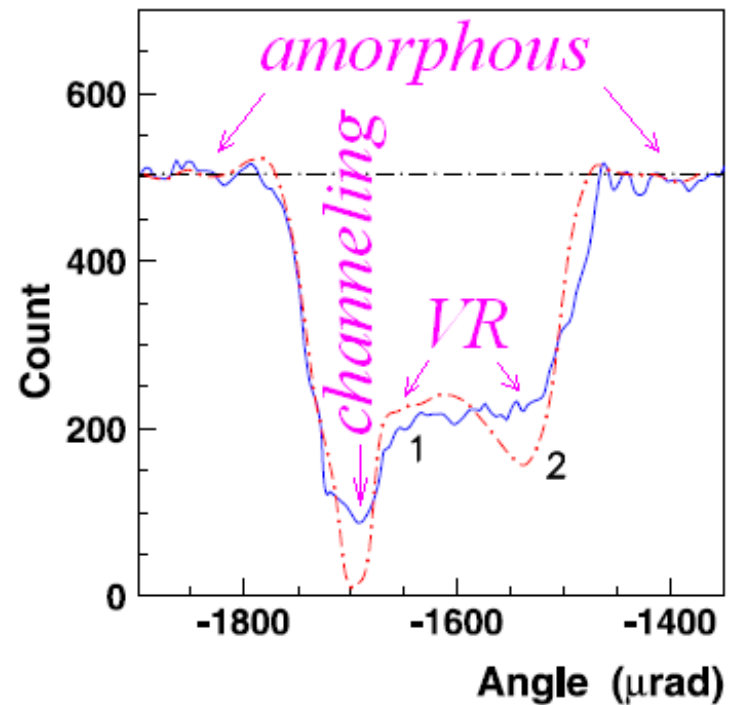
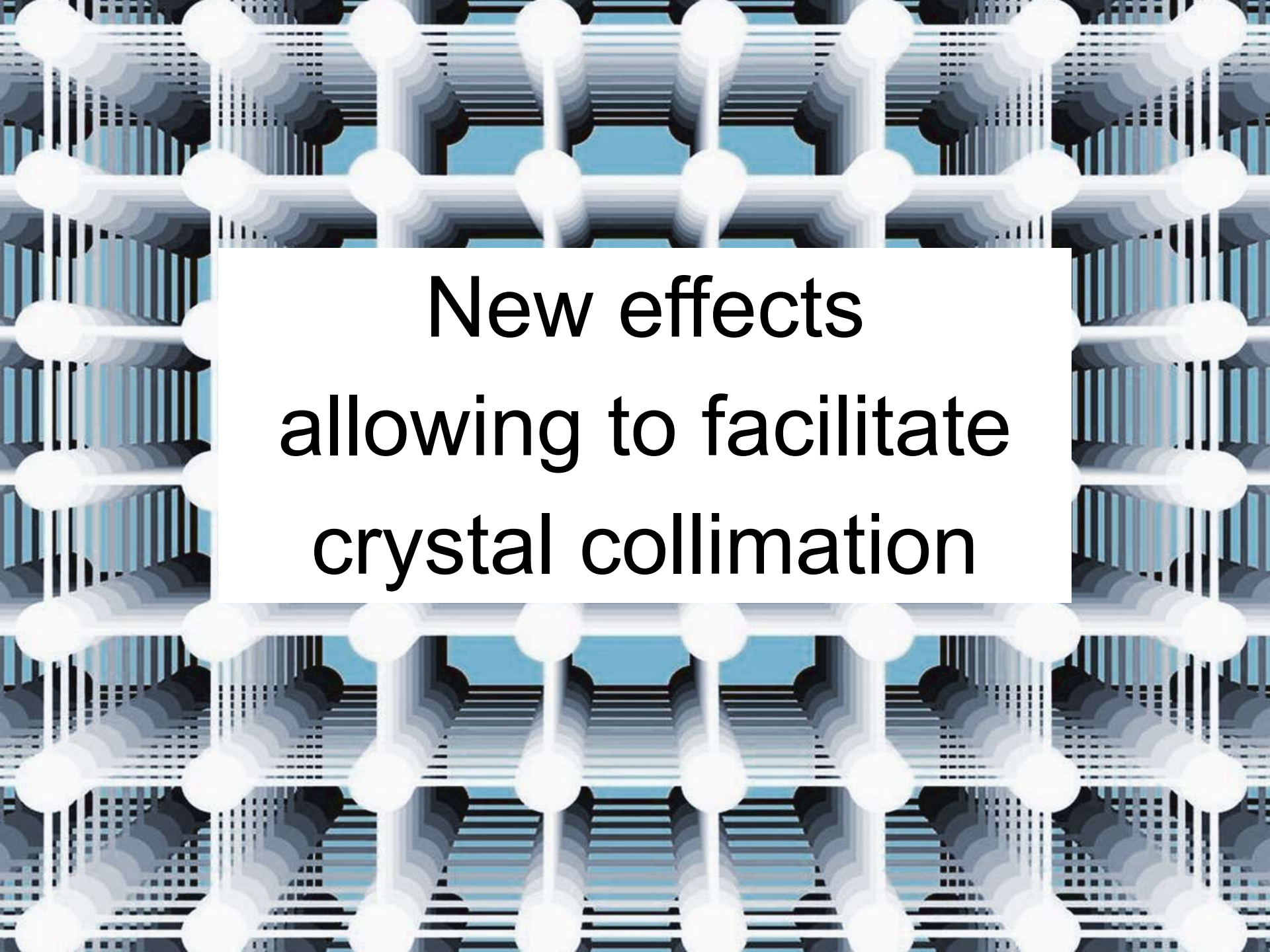


Fig. 3. (Color online.) (1) The dependence of the S1-S2 telescope count on the angular position of the crystal 1; (2) The dependence of the number of inelastic nuclear interactions of protons in the crystal on its orientation angle obtained by simulation. The dot-dashed line shows the level of the beam losses for the amorphous orientation of the crystal.

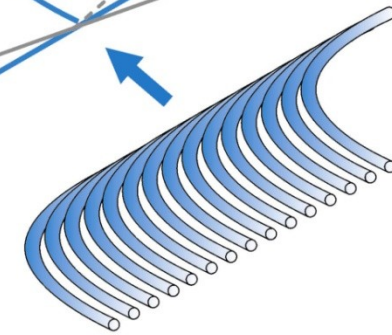
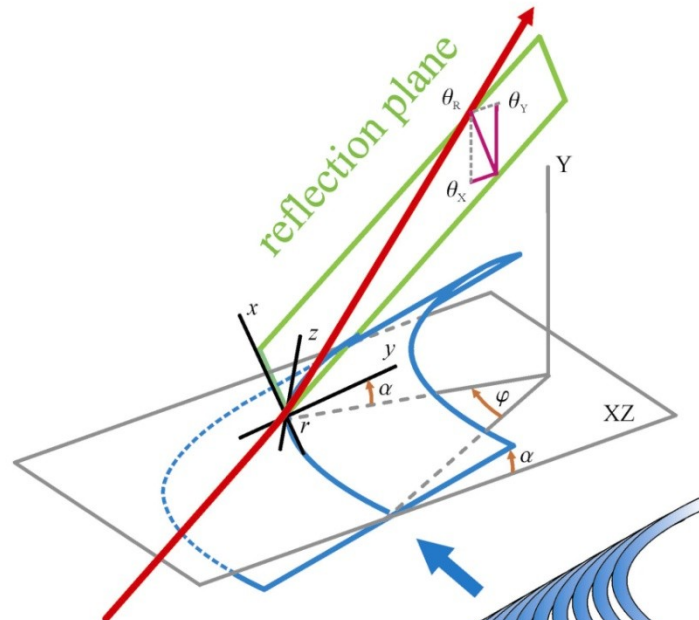
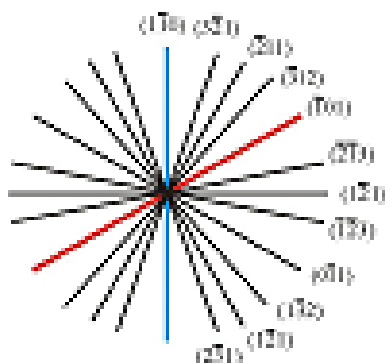
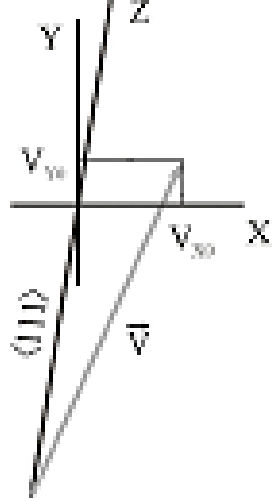
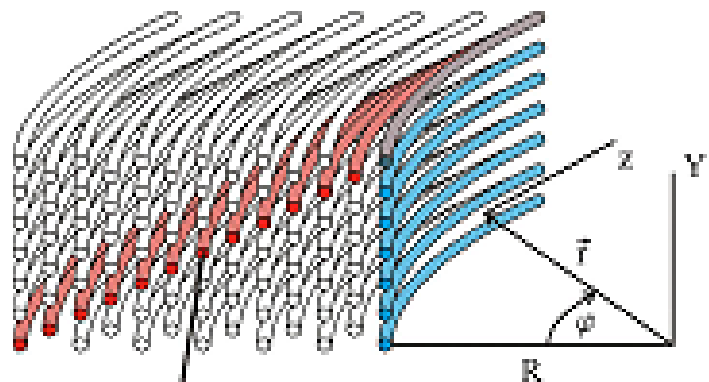


New effects
allowing to facilitate
crystal collimation

Multiple **V**olume
Reflection from
different inclined
planes of **O**ne **C**rystal
(MVROC)

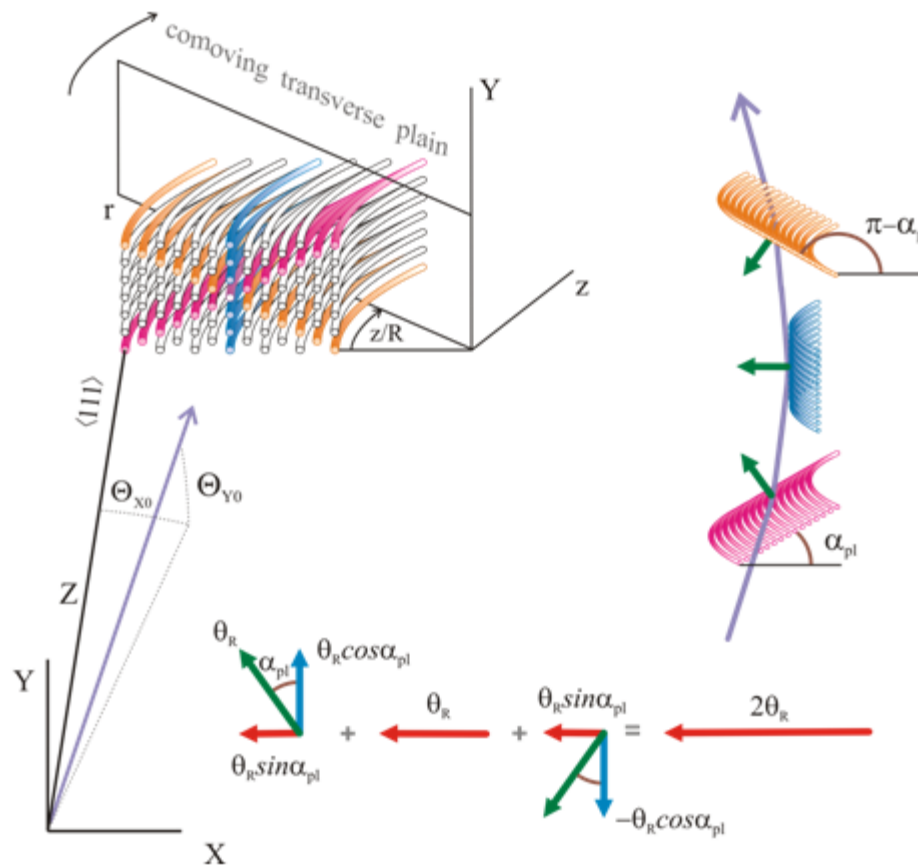
Multiple Volume Reflection in One Crystal (MVROC)

V.V. Tikhomirov, PLB 655(2007)217



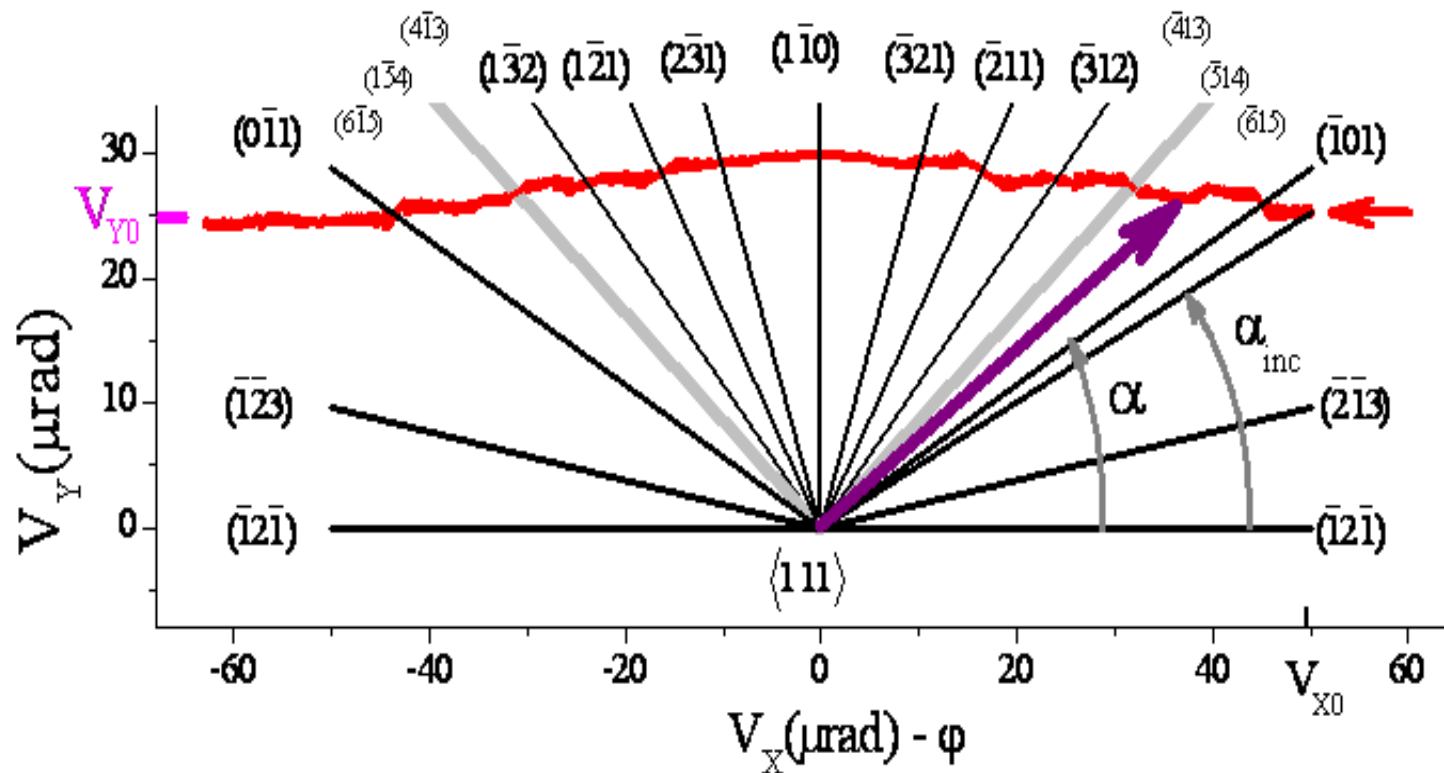
Axes form **many** inclined reflecting planes

Horizon projections of the angles of reflection from different skew planes sum up giving rise to the MVROC effect while the vertical angles of reflection from symmetric skew planes, like (-101) and (0-11), mutually compensate.



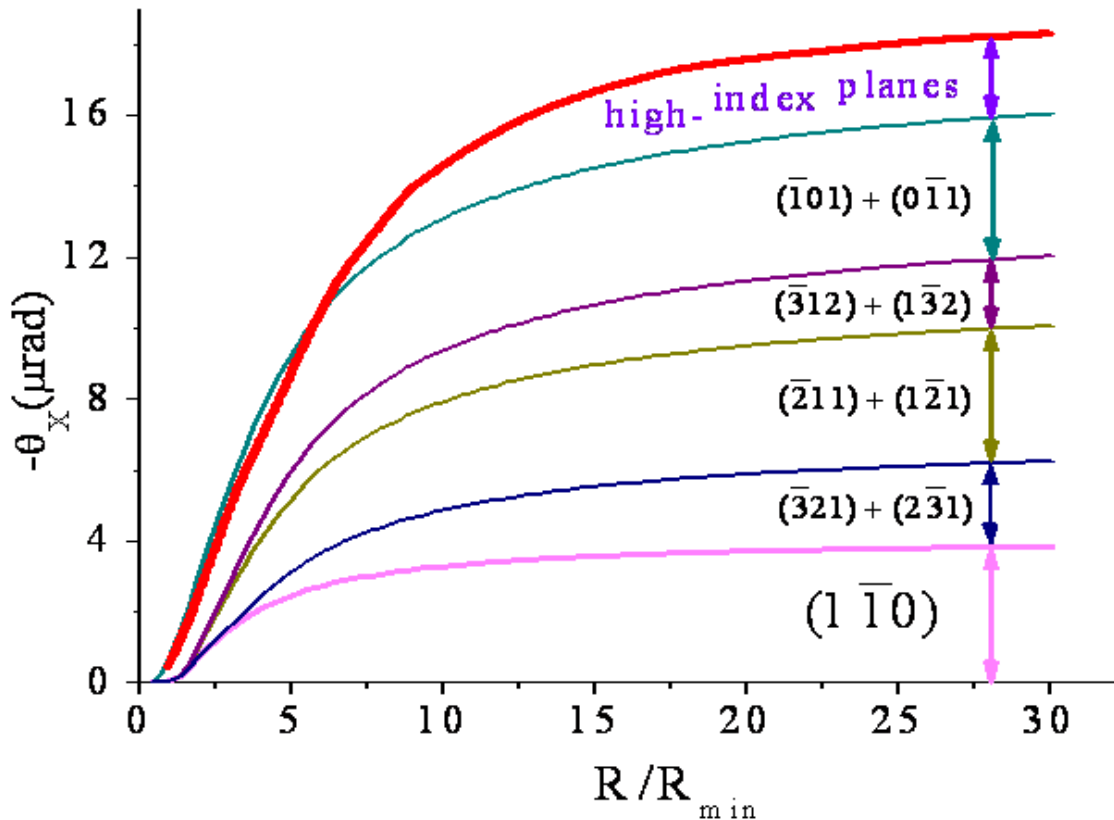
Comoving reference frame rYz rotates with the normal bent axis direction when a particle moves through the crystal.

Proton motion in comoving reference plane



Protons are reflected from **many** different crystal plane sets in **one** crystal

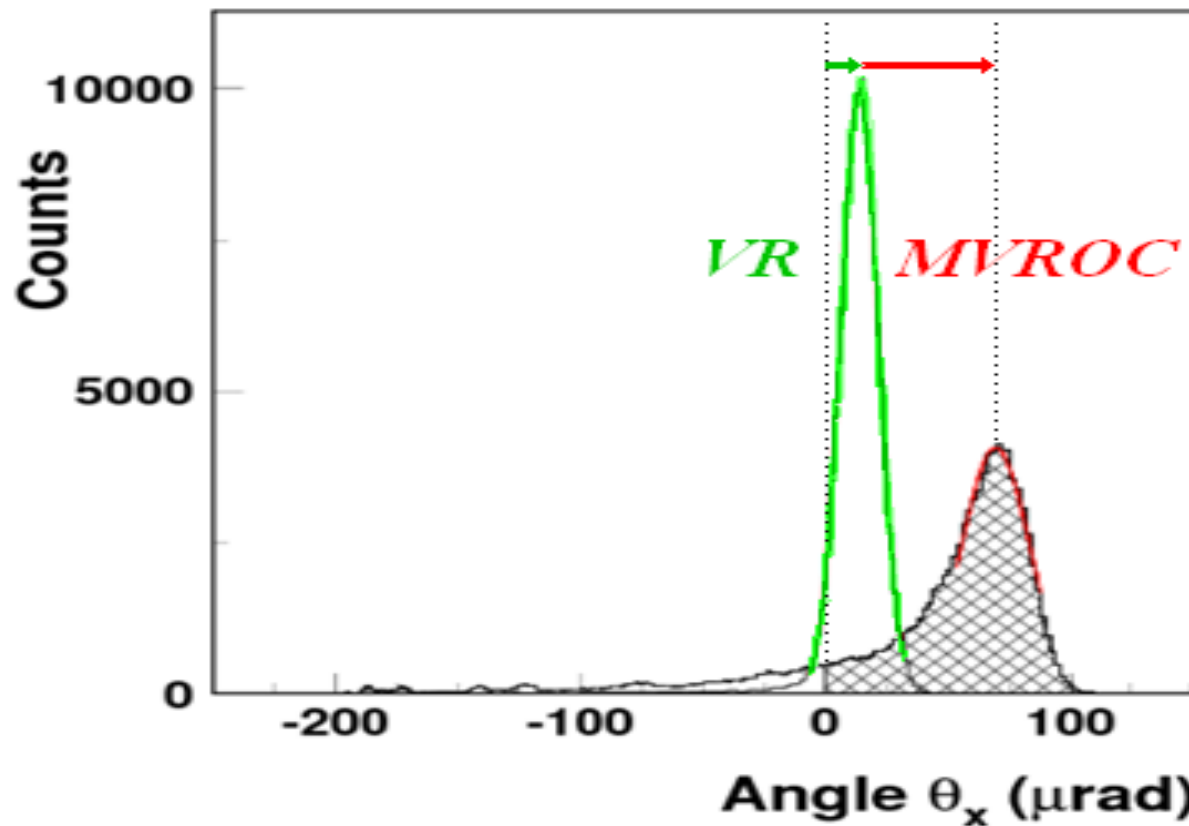
Reflection angles from planes of one crystal vs bending radius



Reflection from different crystal planes increases VR angle about **5 times**

First MVROC observation

W. Scandale et al, PLB 682(2009)274



MVROC indeed increases reflection angle **5 times**

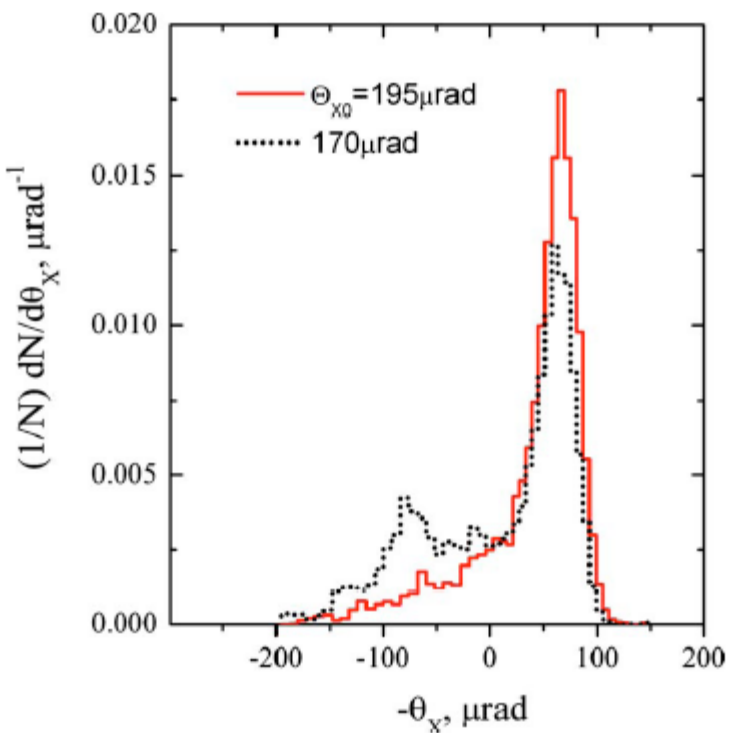


FIG. 8. (Color online) Simulated proton angular distributions in the horizontal plane under the conditions of experiment (Ref. 13) at horizontal incidence angles $\Theta_{x0}=170$ and $195 \mu\text{rad}$. The peak in the region of $\theta_x \approx 85 \mu\text{rad}$ is formed by the protons captured into the channeling regime by (101) plane at the crystal surface at $\Theta_{x0}=170 \mu\text{rad}$.

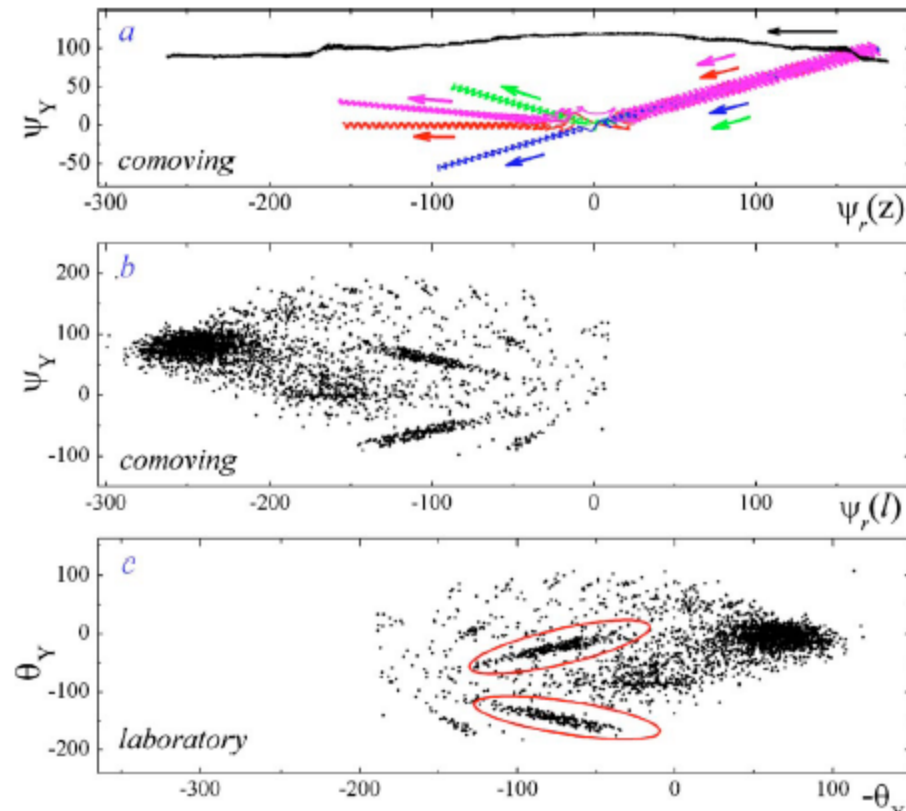


FIG. 7. (Color online) Evolution of the proton deflection angles with crystal depth in the comoving reference frame: one proton experiences MVROC (top) while the other four are first captured by $\langle\bar{1}01\rangle$ planes, then scattered by $\langle111\rangle$ axes and finally recaptured by various crystal planes (a). Proton angular distribution behind the crystal in comoving (b) and laboratory (c) reference frames. All the angles are measured in microradians. Both crystal and beam parameters correspond to the conditions of the experiment (Ref. 13).

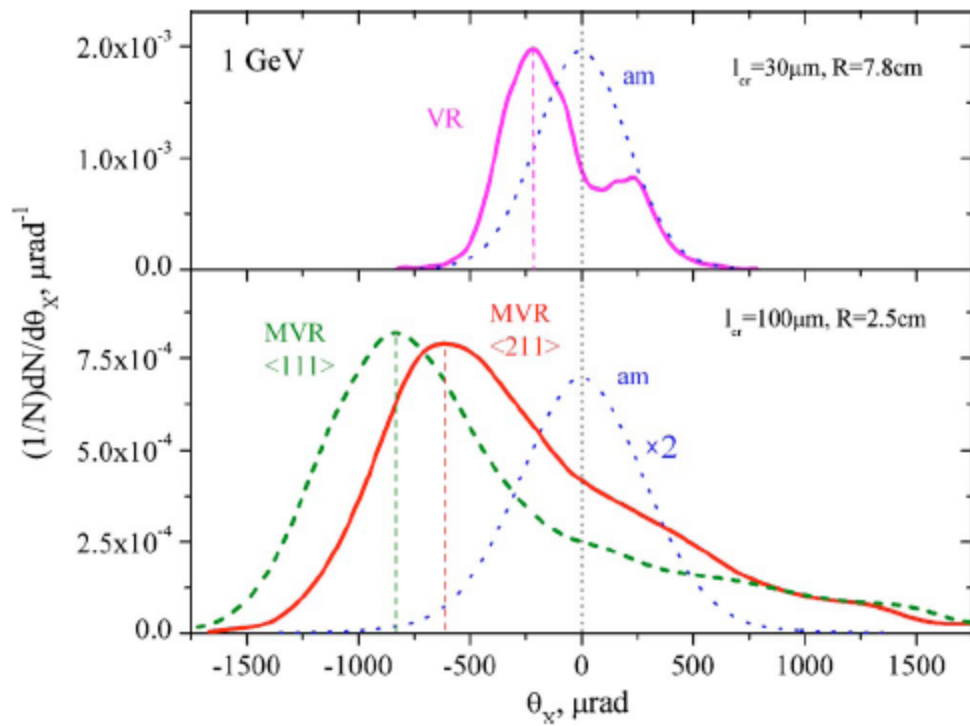


FIG. 3. (Color online) Angular distributions of 1 GeV protons undergoing VR in $30 \mu\text{m}$ Si(211) crystal bent with $R = 7.8 \text{ cm}$ at $\Theta_{X0}=0.294 \text{ mrad}$ and $\Theta_{Y0}=4 \text{ mrad}$ (top) and MVR in $100 \mu\text{m}$ Si crystal bent with $R = 2.5 \text{ cm}$ at $\Theta_{X0}=2 \text{ mrad}$ and $\Theta_{Y0}=1 \text{ mrad}$ (bottom). Solid line for $\langle 211 \rangle$ and $\Theta_{Y0}=1 \text{ mrad}$, dashed line for $\langle 111 \rangle$ and $\Theta_{Y0}=0.8 \text{ mrad}$. Dotted Gaussian bells correspond to scattering by an amorphous medium.

Guidi, Mazzolari, and Tikhomirov J. Appl. Phys. 107, 114908 (2010)

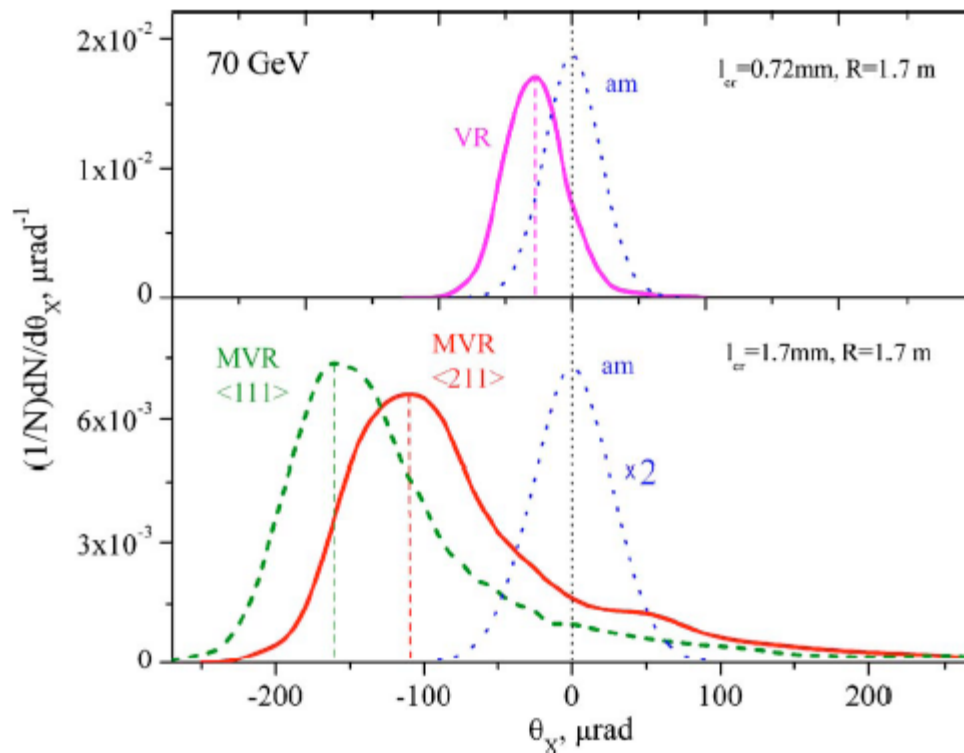


FIG. 4. (Color online) Angular distributions of 70 GeV protons undergoing VR in 0.72 mm Si(211) crystal at $\Theta_{x0}=0.211$ and $\Theta_{y0}=2$ mrad (top) and MVROC in 1.7 mm Si crystal at $\Theta_{x0}=0.5$ and $\Theta_{y0}=0.2$ mrad (bottom). Solid line for $\langle 211 \rangle$ and dashed line for $\langle 111 \rangle$, $R=1.7$ m in all cases.

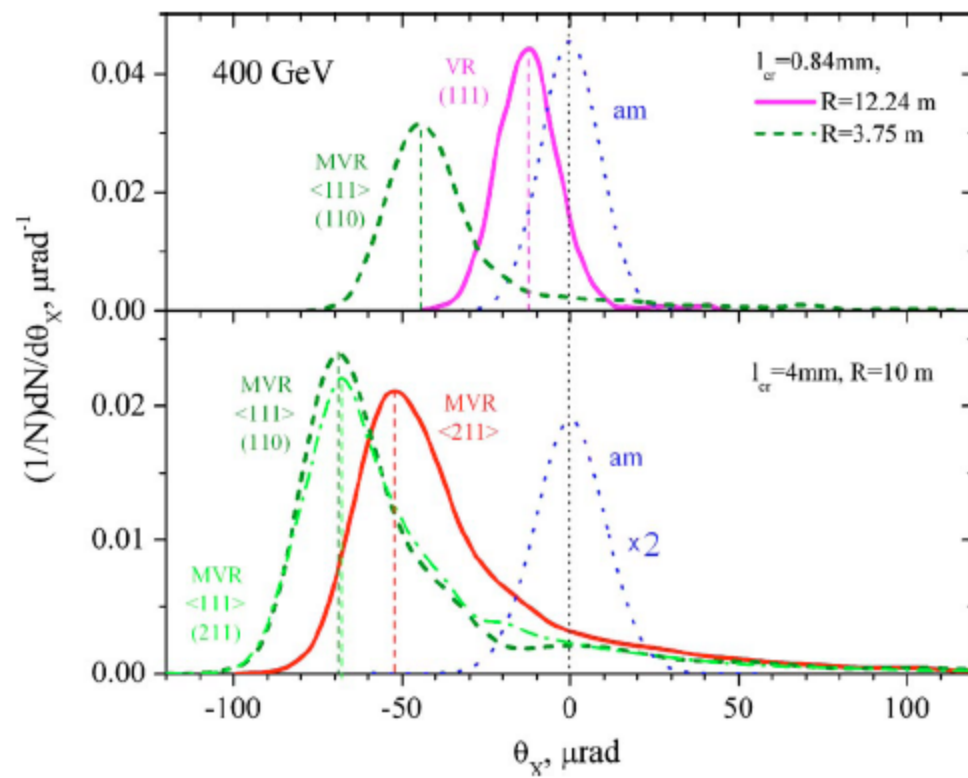


FIG. 5. (Color online) Angular distributions of 400 GeV protons experiencing VR at $R=12.24\text{ m}$, $\Theta_{x0}=35.5\text{ }\mu\text{rad}$, $\Theta_{y0}=0.5\text{ mrad}$ and MVROC at $R=3.75\text{ m}$, $\Theta_{x0}=100$, $\Theta_{y0}=37.5\text{ }\mu\text{rad}$ in 0.86 mm Si(111) crystal (top) and MVROC at $R=10\text{ m}$, $\Theta_{x0}=200$ and $\Theta_{y0}=75\text{ }\mu\text{rad}$ in 4 mm Si crystal (bottom). Solid line for $\langle 211\rangle$, dashed one for $\langle 111\rangle$, $\langle 110\rangle$ plane vertical, and dash-dot one for $\langle 111\rangle$, $\langle 211\rangle$ plane vertical.

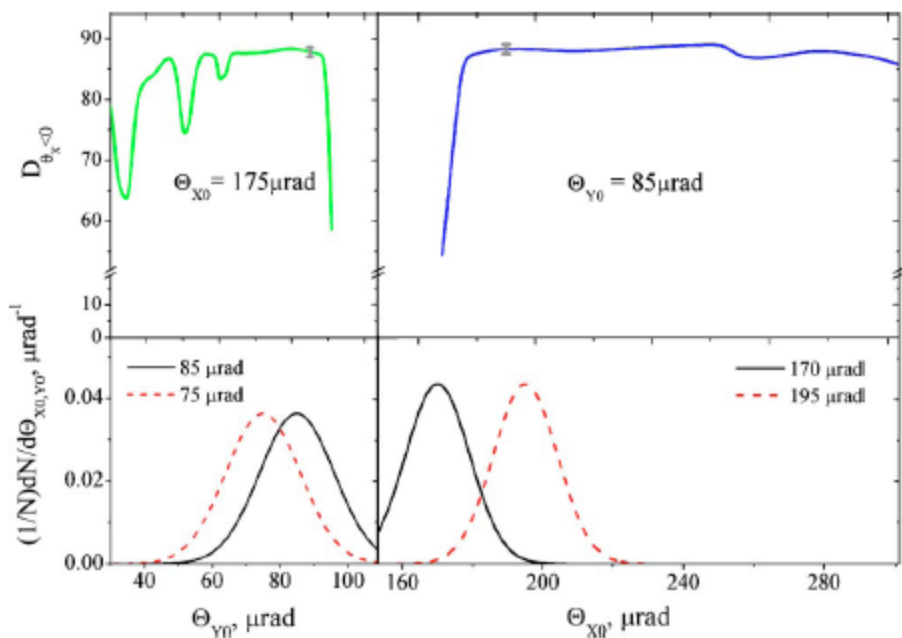


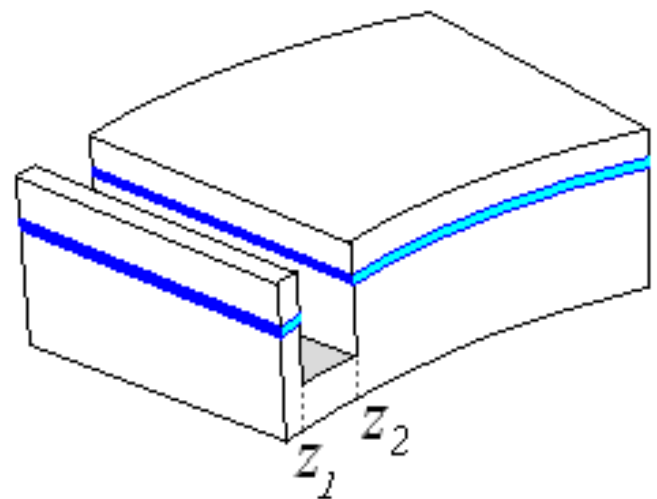
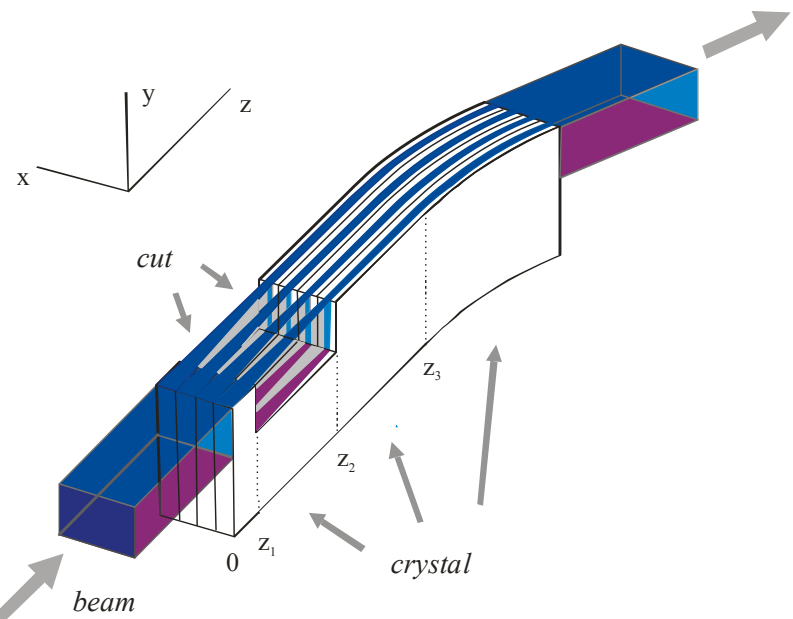
FIG. 6. (Color online) Top: probability of 400 GeV proton deflection in 4 mm Si crystal bent with $R=11.43$ m vs vertical incidence angle with the horizontal one fixed at $175 \mu\text{rad}$ (left) and vs the horizontal incidence angle with the vertical one fixed at $85 \mu\text{rad}$ (right). Bottom: proton angular distributions in vertical (left) and horizontal (right) planes under the conditions of experiment (Ref. 13).

Channeling fraction increase by **crystal cut**

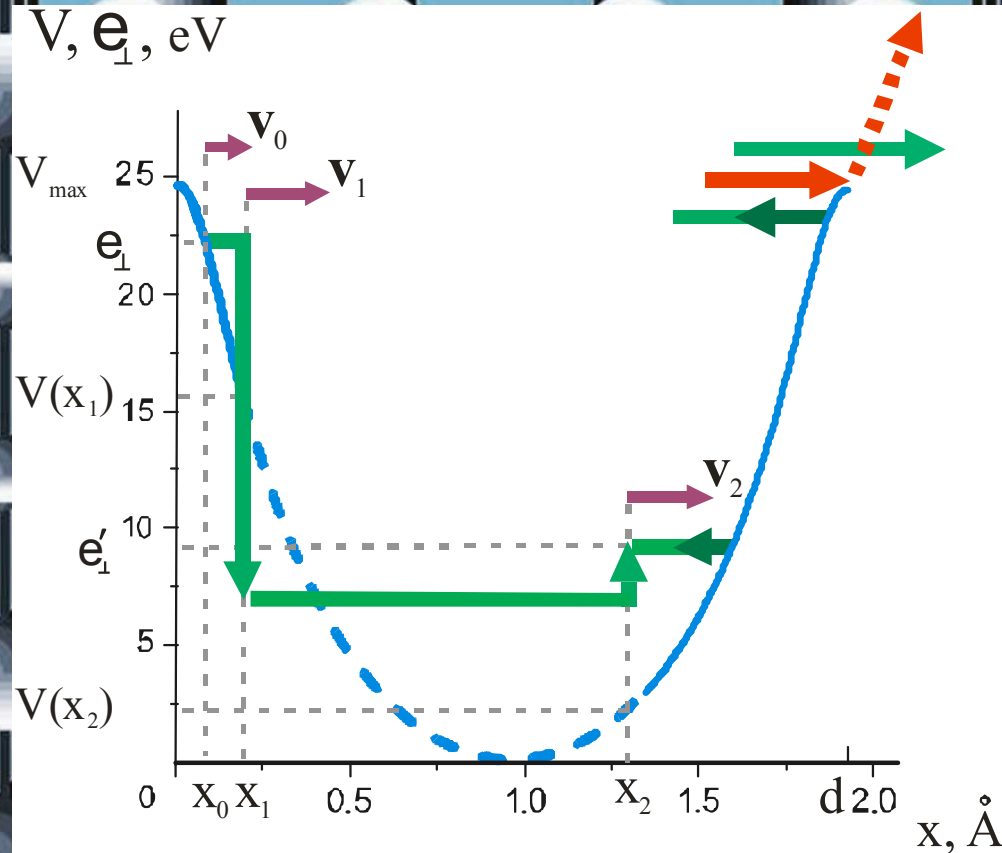
or buried amorphous layer

The capture probability **increase** by crystal cut

V.V.Tikhomirov, JINST, 2(2007)P08006

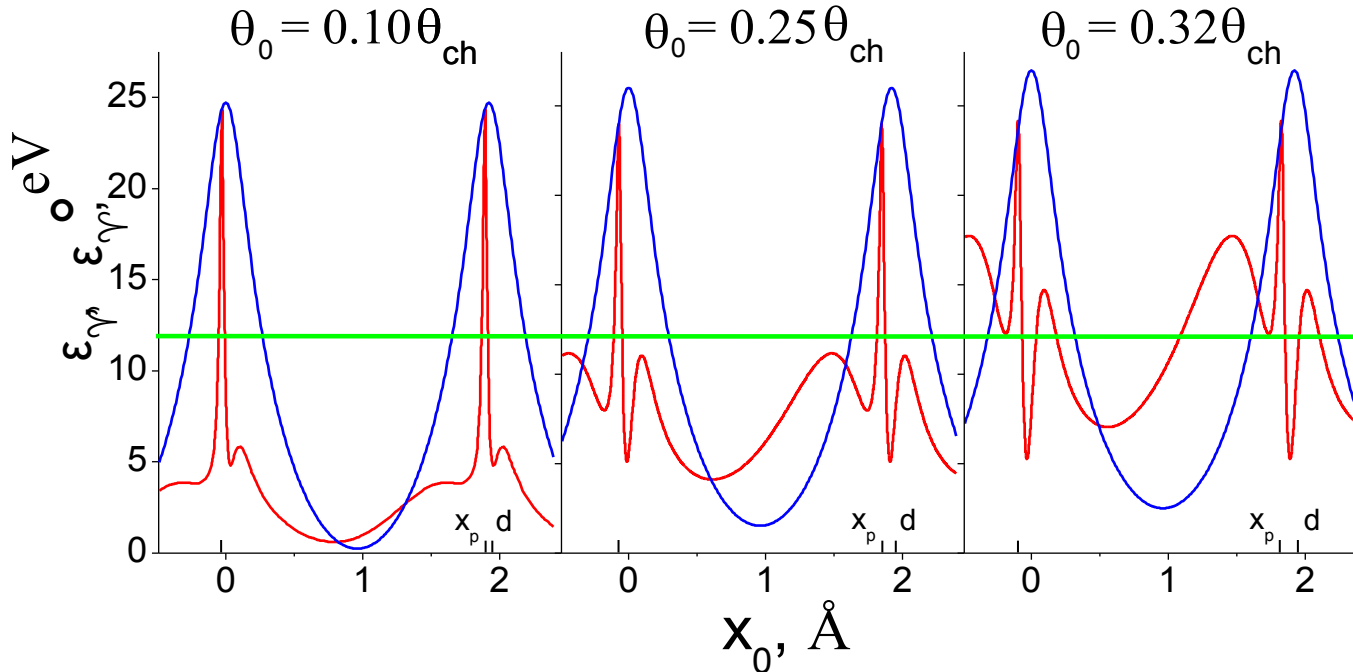


Transverse energy reduction *by the cut - 1*



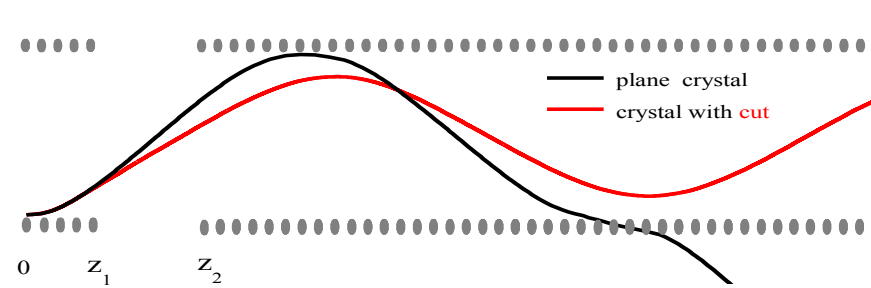
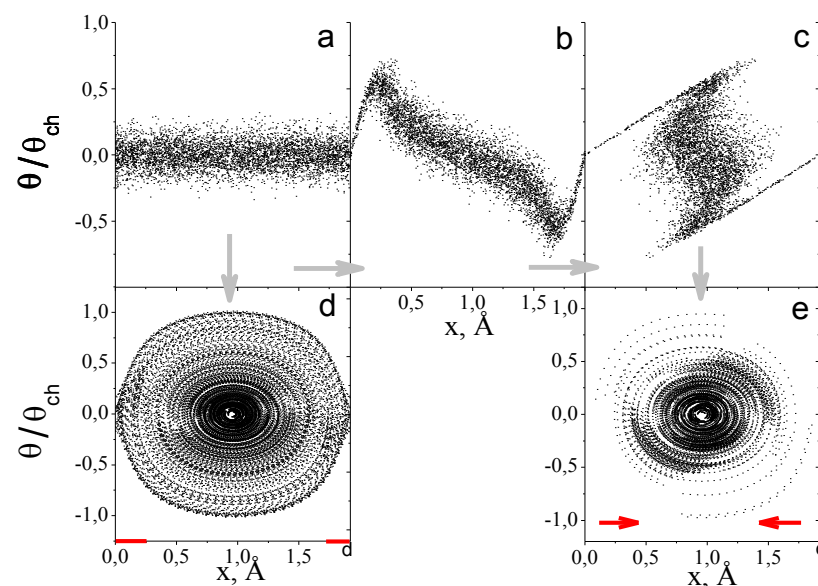
The cut diminishes the potential energy conserving the transverse kinetic one

Transverse energy reduction *by the cut - 2*



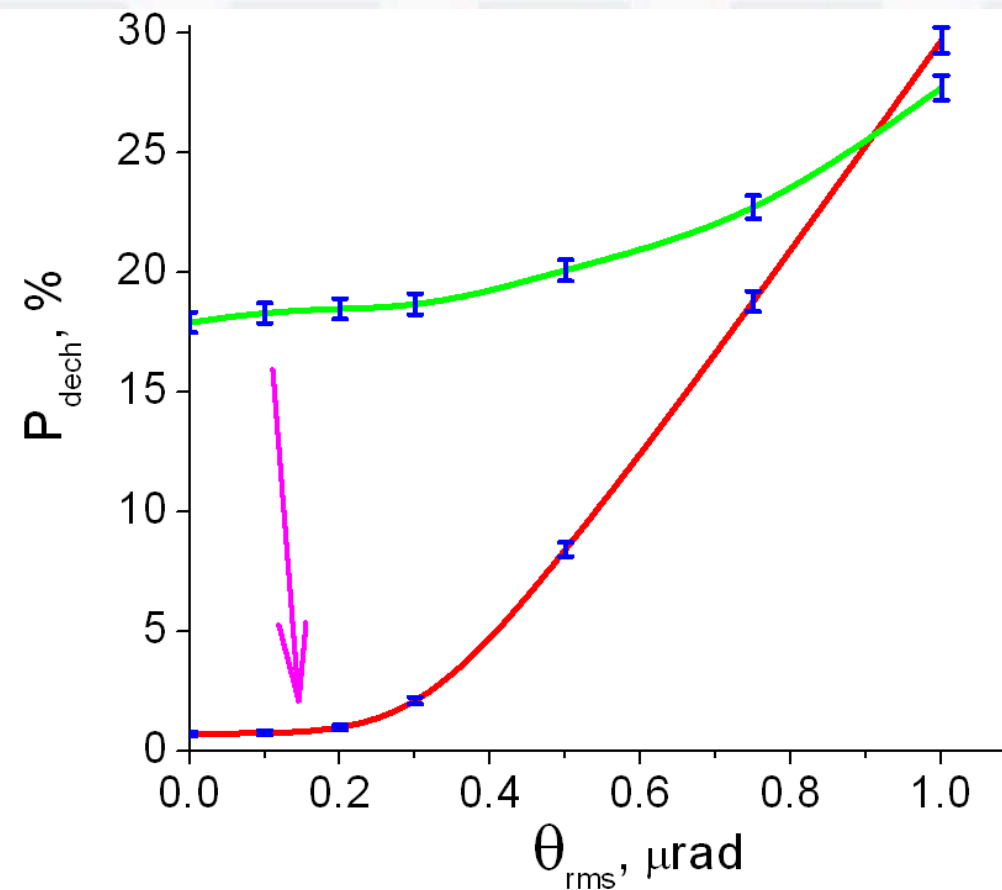
Only 1-2% of protons avoid drastic transverse energy reduction by the cut

Phase space transformation by the cut



Protons cease to reach the high nuclear density **regions**

Channeling fraction increase by the cut



The cut increases channeling fraction **from 85 to 99%**

Cut formation method

(110) Silicon Etching for High Aspect Ratio Comb Structures

*Seong-Hyok Kim, Sang-Hun Lee, Hyung-Taek Lim, and Yong-Kweon Kim

School of Electrical Engineering, Seoul National University

San 56-1 Shilim-dong, Kwanak-gu, Seoul, 151-742, Korea

Seung-Ki Lee

Department of Electrical Engineering, Dankook University

8, Hannam-dong, Yongsan-gu, Seoul 140-714, Korea

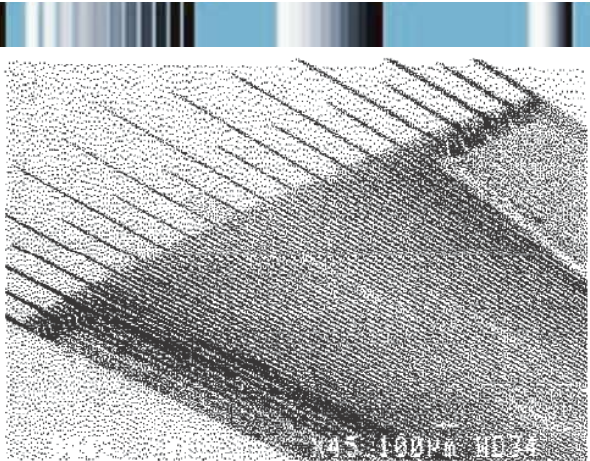


Fig. 1. SEM photograph of alignment target after
wet etching

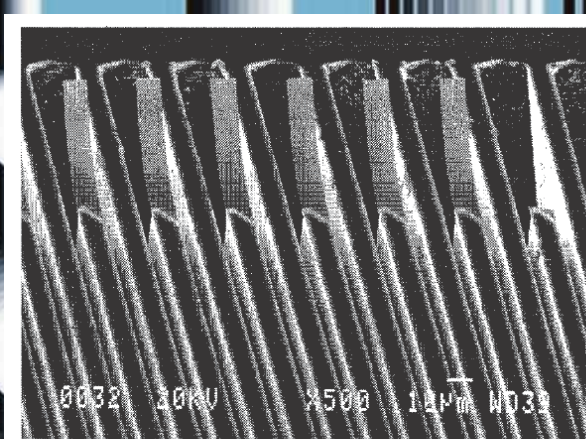
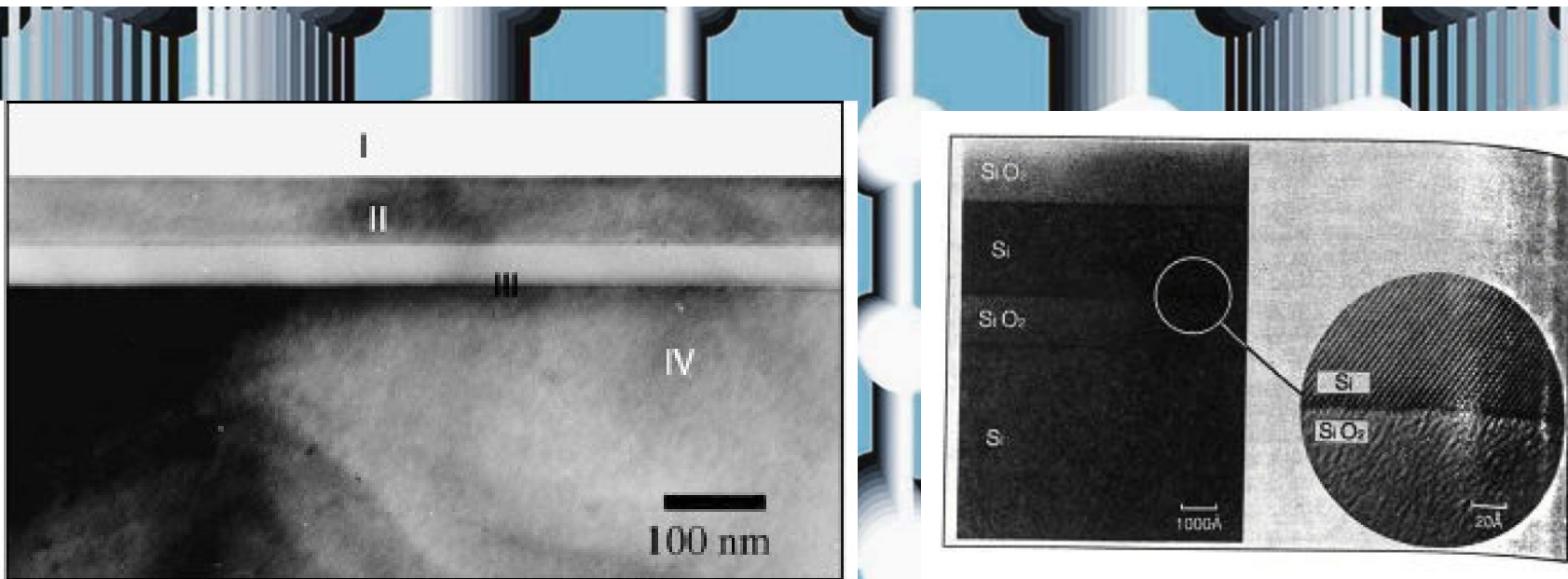


Fig. 12 Fabricated comb structures.
The width is 8 μ m, gap is 7 μ m and height is about 150 μ m

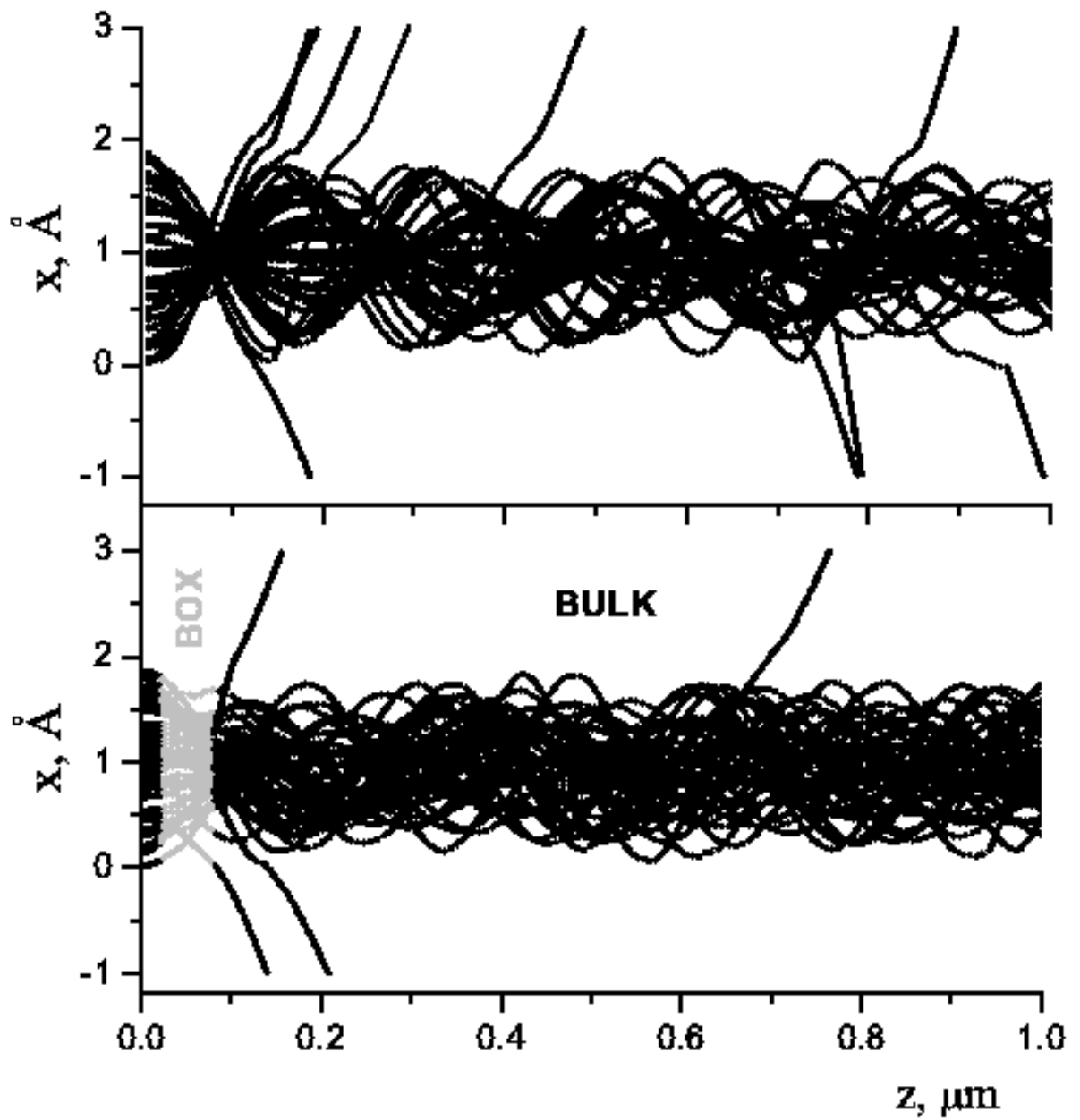
Crystal cut can be produced by
anisotropic etching

SIMOX Buried Oxide Layer can be used instead of crystal cut

V. Guidi, A. Mazzolari and V.V. Tikhomirov, *J. Phys. D: Appl. Phys.* 42(2009) 165301



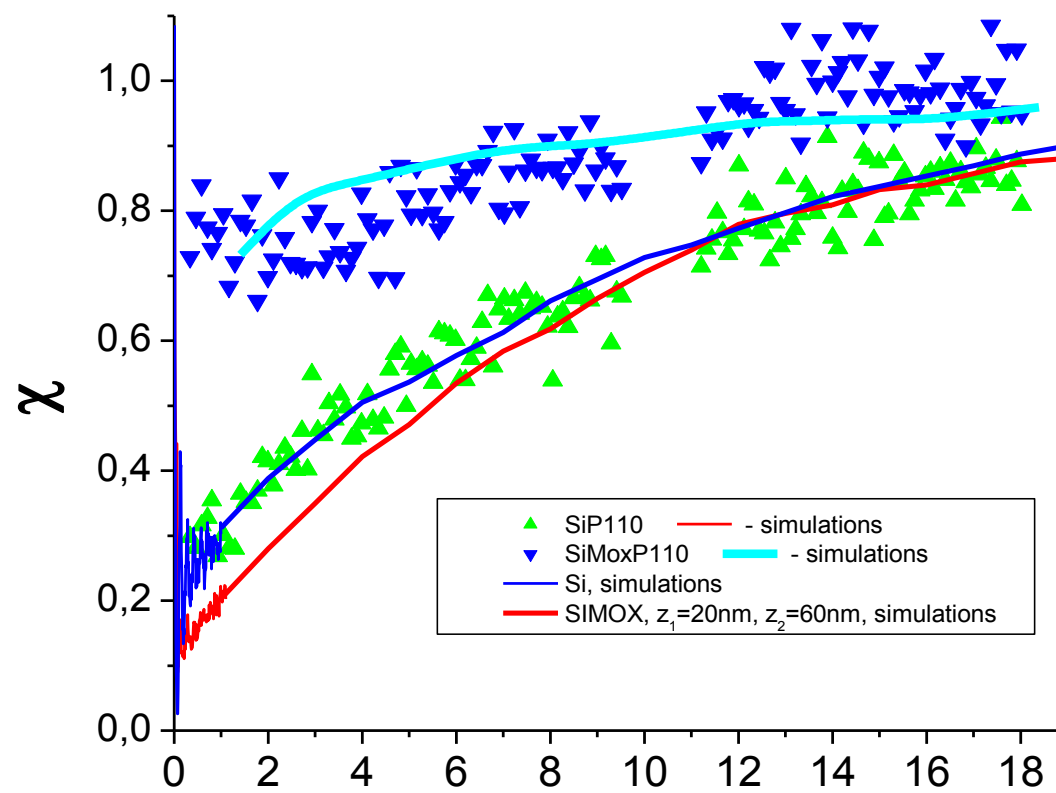
- Thermal annealing restores silicon crystalline quality and creates a buried SiO₂ layer,
- Interfaces between Si and SiO₂ are well terminated,
- Misalignment between silicon layers in available SIMOX structures: less than 0.7 Å/mm.



BOX layer
“focuses”
protons
like a *cut*
diminishing
their
transverse
energy

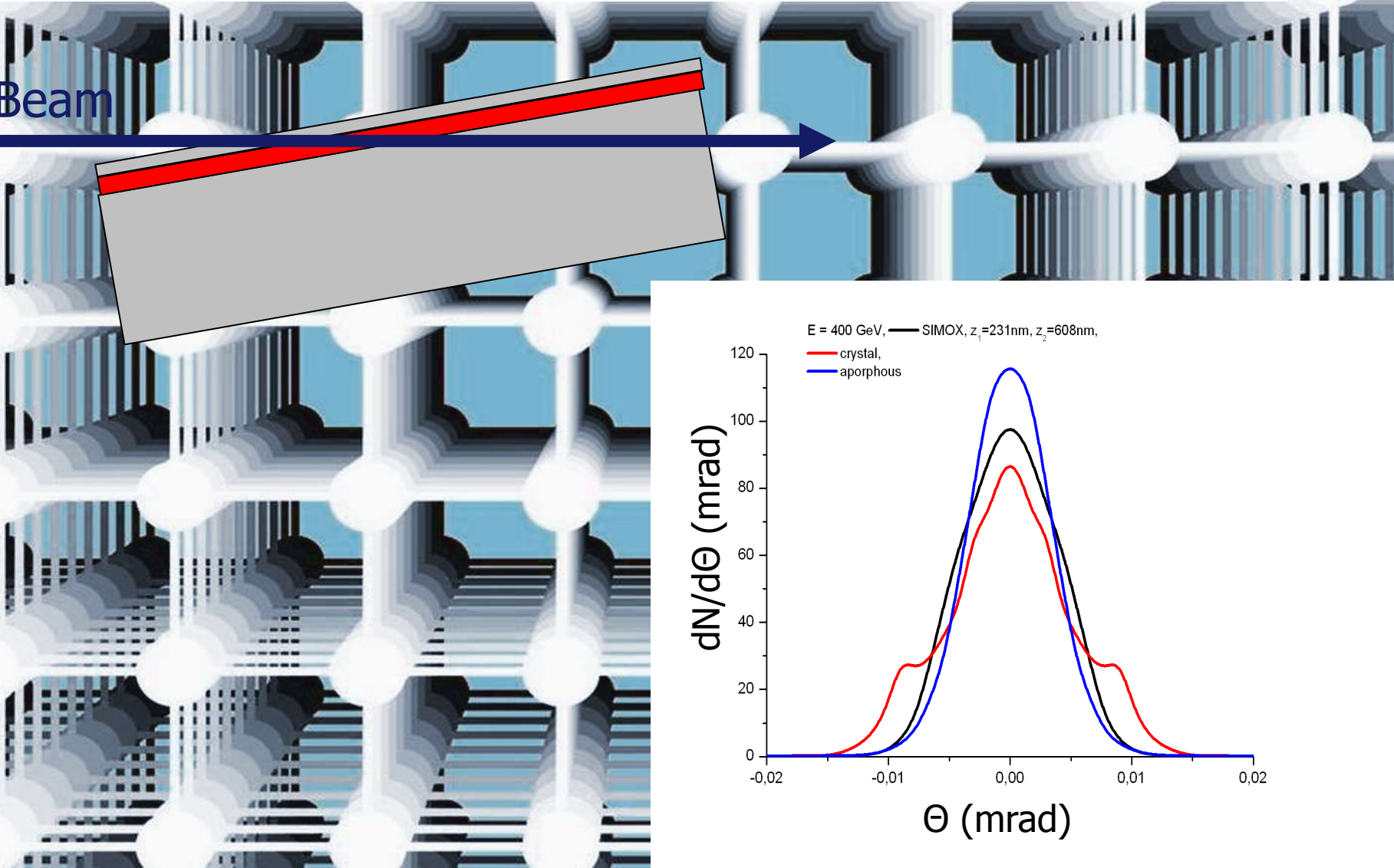
$$\begin{aligned} z_1 &= 20 \text{ nm}, \\ z_2 &= 80 \text{ nm}, \\ z_3 &= 1 \text{ } \mu\text{m}, \\ E_p &= 7 \text{ MeV} \end{aligned}$$

Rutherford Backscattering
allows to observe
the channeling efficiency increase
at low energies (6.1 MeV Legnaro)

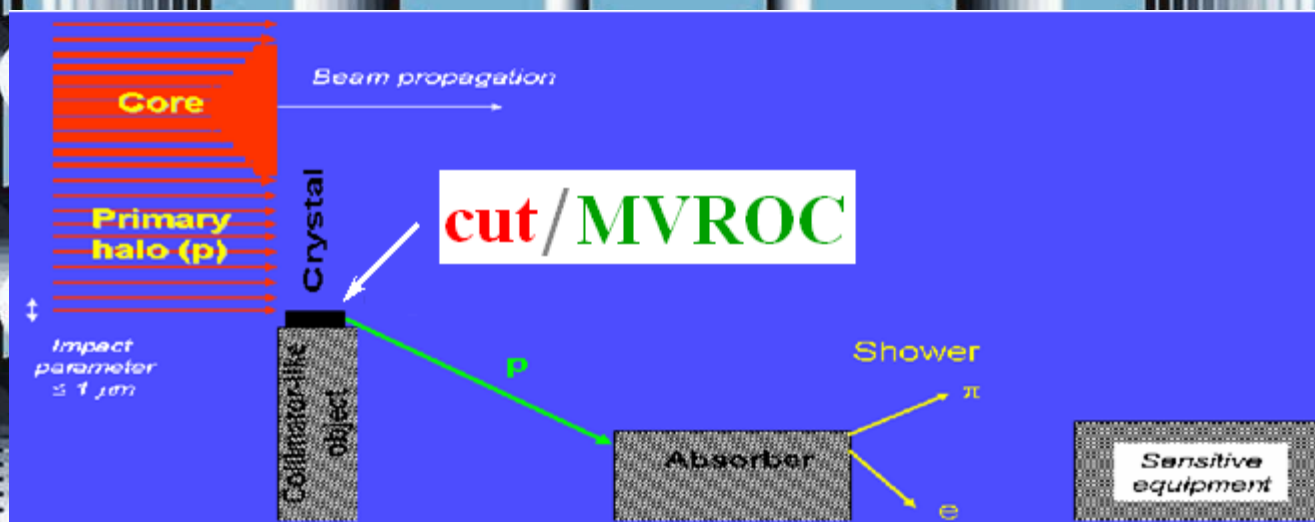


Grazing proton incidence allows to observe
the channeling efficiency increase
at SPS energy of 400 GeV (H8 line)

Beam

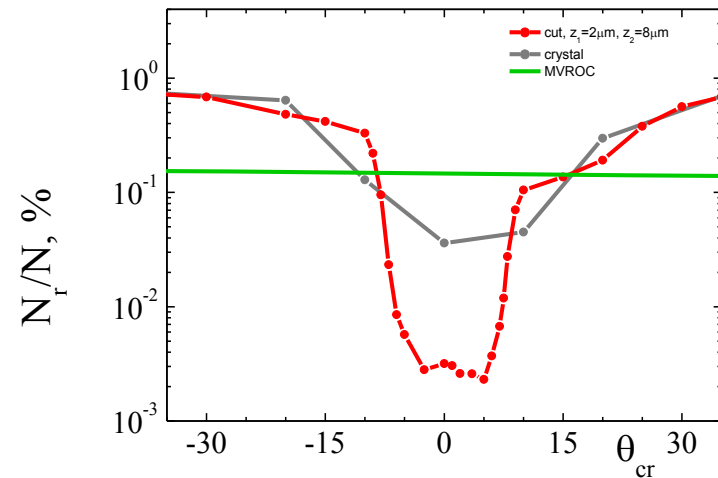
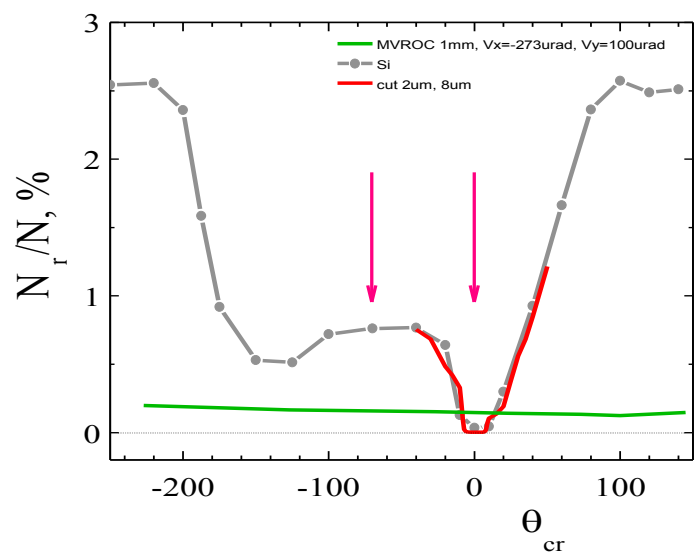


Crystal cut and MVROC application to crystal collimation



Inelastic loss fraction as a function of the crystal orientation

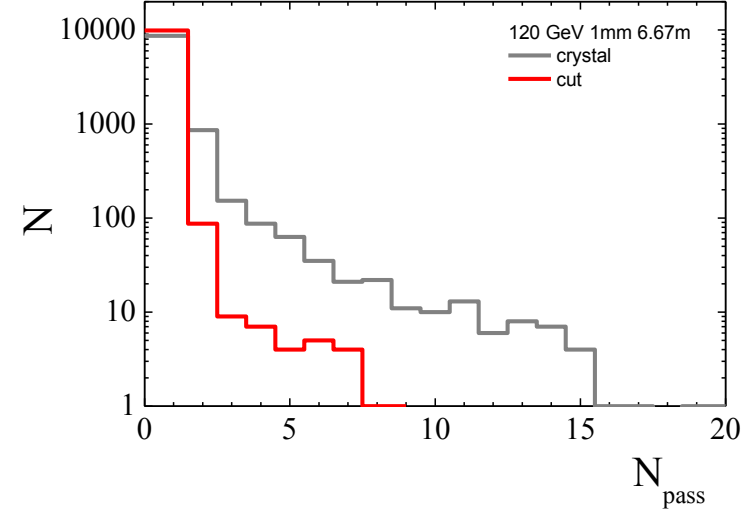
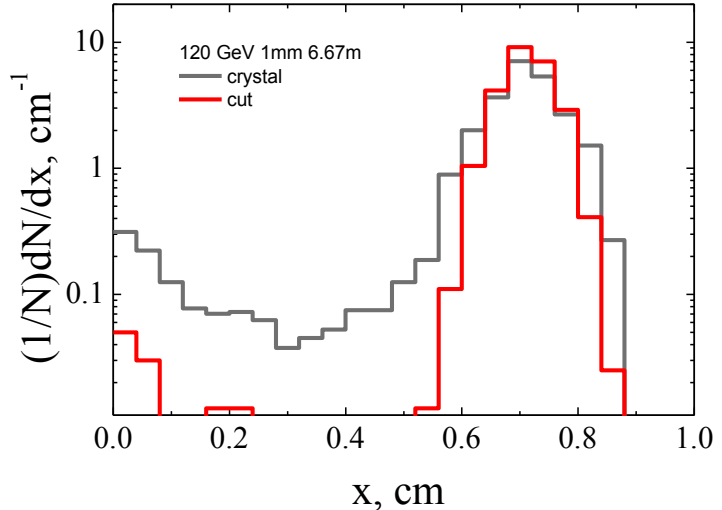
in the usual crystal, **crystal with cut** and a **crystal in MVROC orientation^{*)}**



Crystal cut decreases inelastic losses
MVROC increases angular acceptance

^{*)} MVROC orientation with $\Theta_{X0} = -273\text{urad}$, $\Theta_{Y0} = 100\text{urad}$ and $R=2\text{m}$

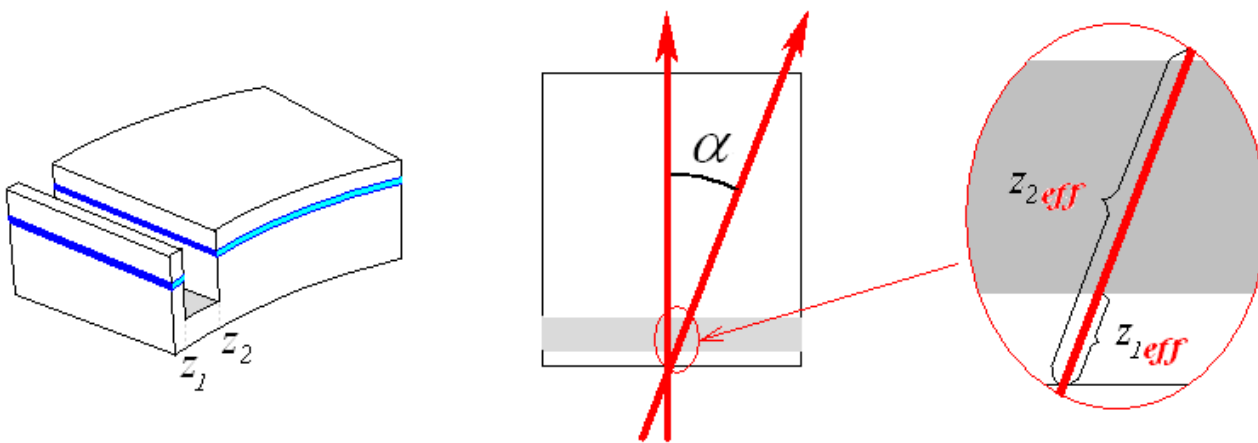
Distributions of the impact parameter and number of the crystal transversals in usual Si crystal and **crystal with cut^{*}** **at perfect alignment**



The cut both increases the impact parameter and decreases the crystal transversals number *at perfect alignment*

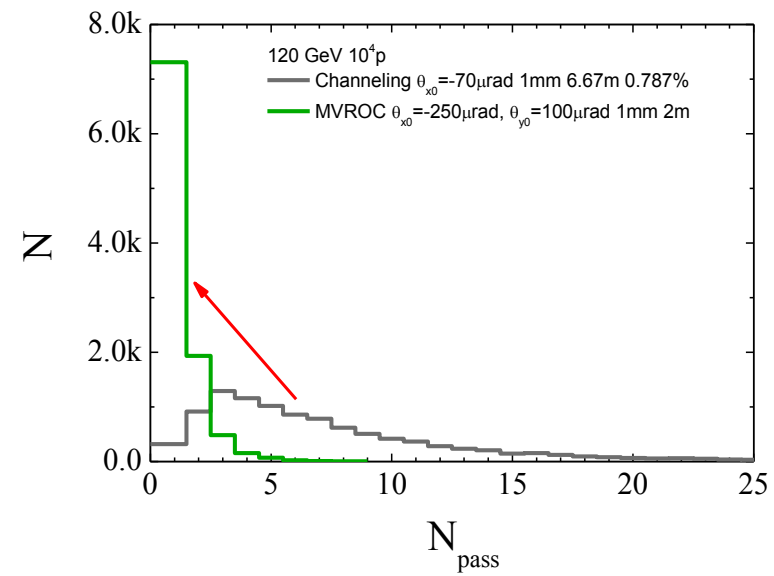
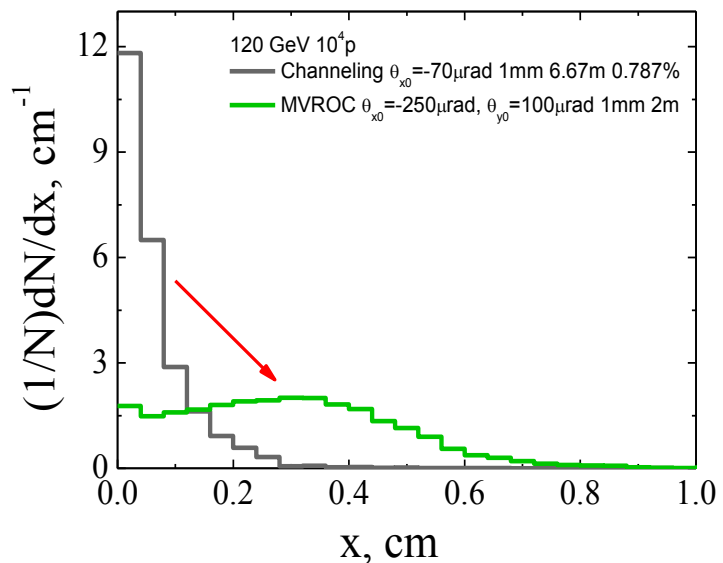
^{*}) cut is between 2 and 8 μm . $R=6.67\text{m}$, $l=1\text{mm}$

Rotation of the crystal with cut allows to use it at ***various energies***



ε, TeV	$z_{1\text{eff}}, \mu\text{m}$	$z_{2\text{eff}} - z_{1\text{eff}}, \mu\text{m}$	R, m	$\alpha, \text{degrees}$
0.45	4.3	14	6.4	0
2	9.1	29	27	62
3.5	12	38	50	69
7	17	54	100	75

Distributions of the impact parameter and number of the crystal transversals in usual Si crystal *) and crystal in MVROC orientation⁺ at rough alignment



MVROC both increases the impact parameter and decreases the crystal transversals number *at rough alignment*

*) $\Theta_{x0} = -70 \mu\text{rad}!$

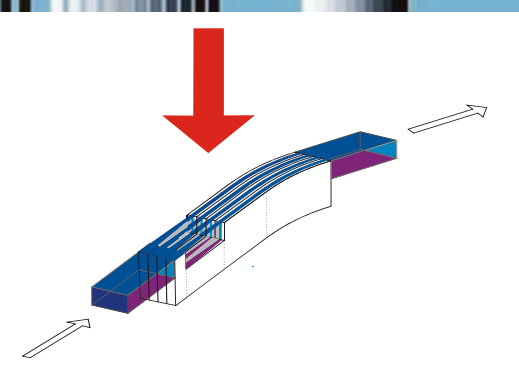
+)
+)
 $\Theta_{x0} = -250 \mu\text{rad}$, $\Theta_{y0} = 100 \mu\text{rad}$ and $R=2\text{m}$

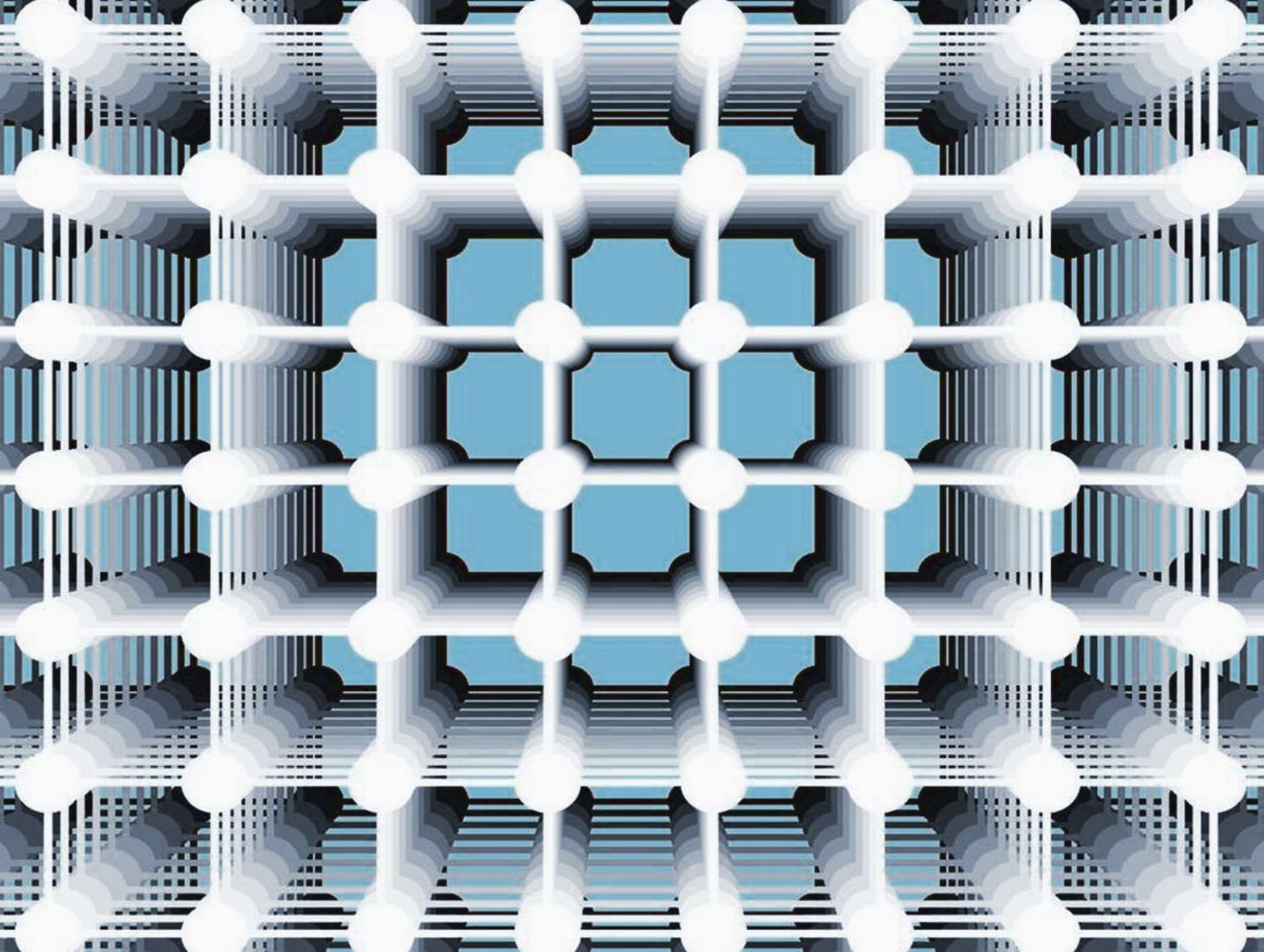
CONCLUSIONS

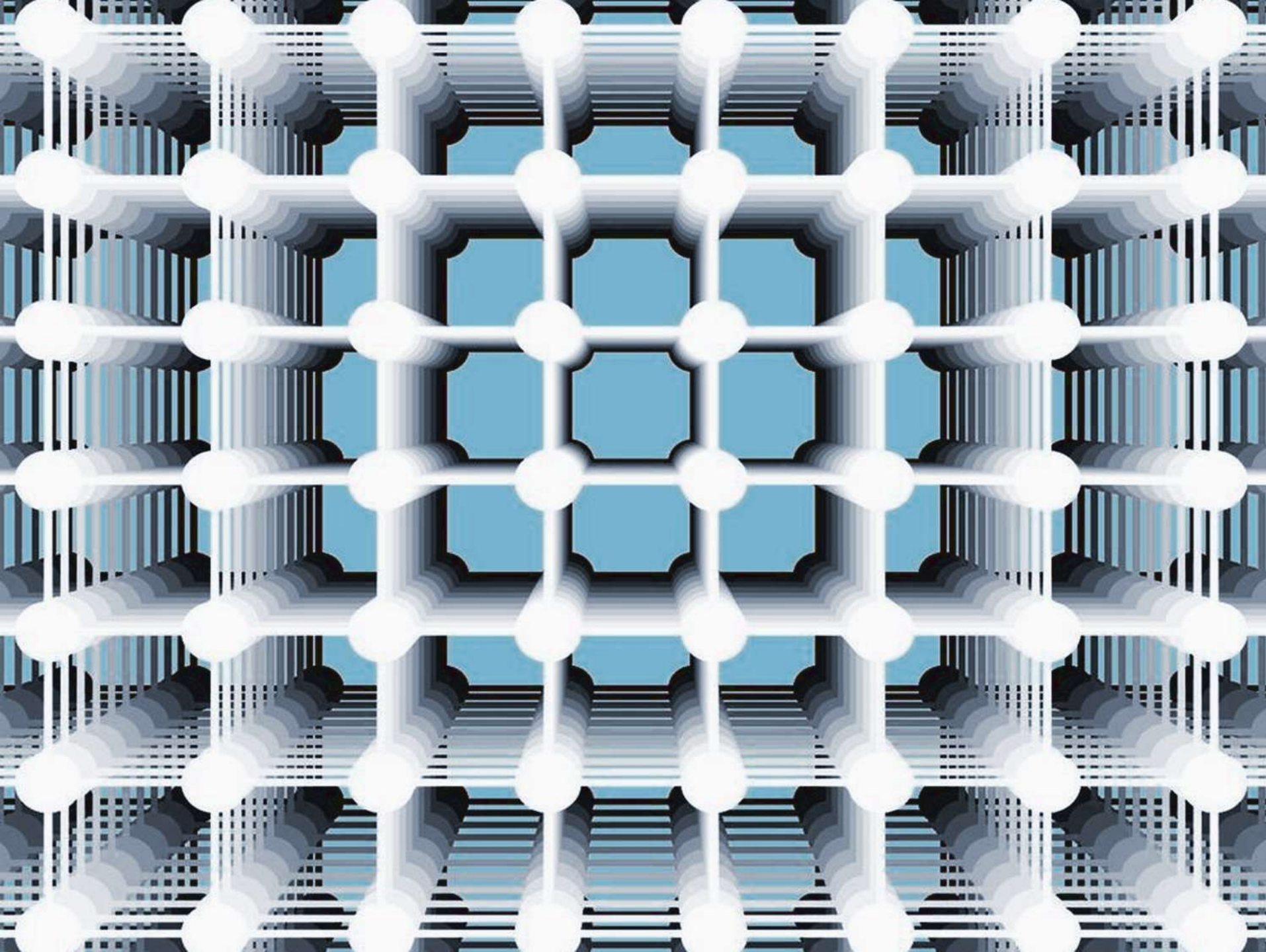
Crystal collimation can be drastically facilitated by both crystal cut and MVROC process, namely:

both the impact parameter can be increased and the crystal transversals number can be decreased

- by crystal cut *at perfect alignment*
- by *MVROC process at rough alignment*

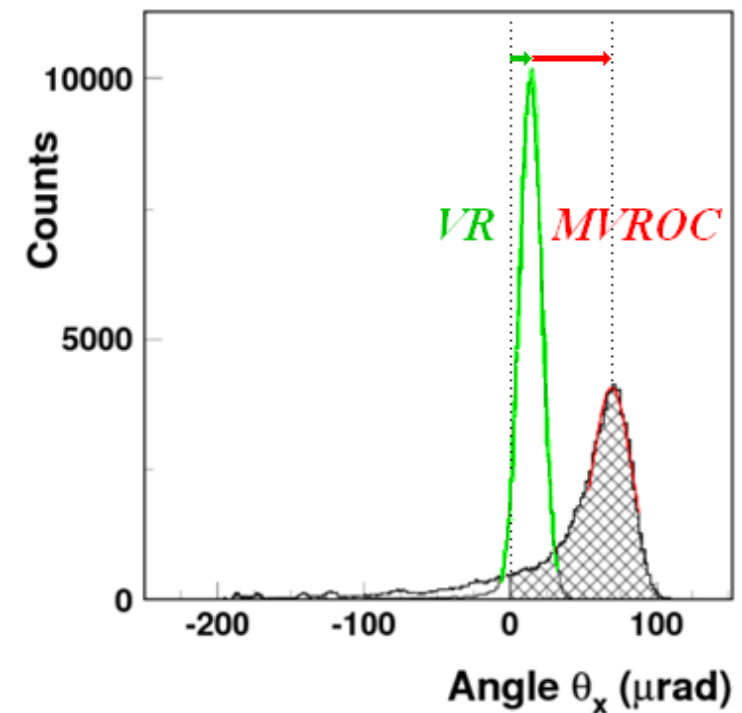
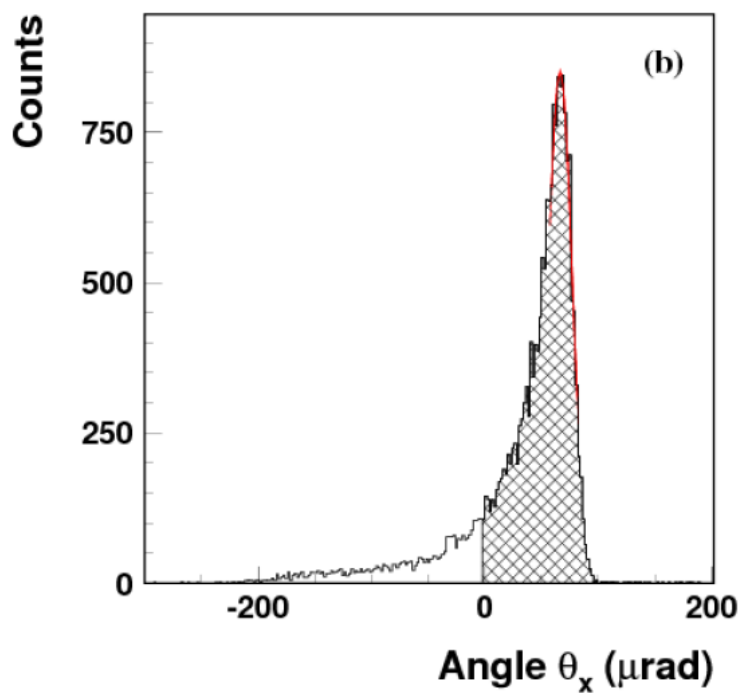






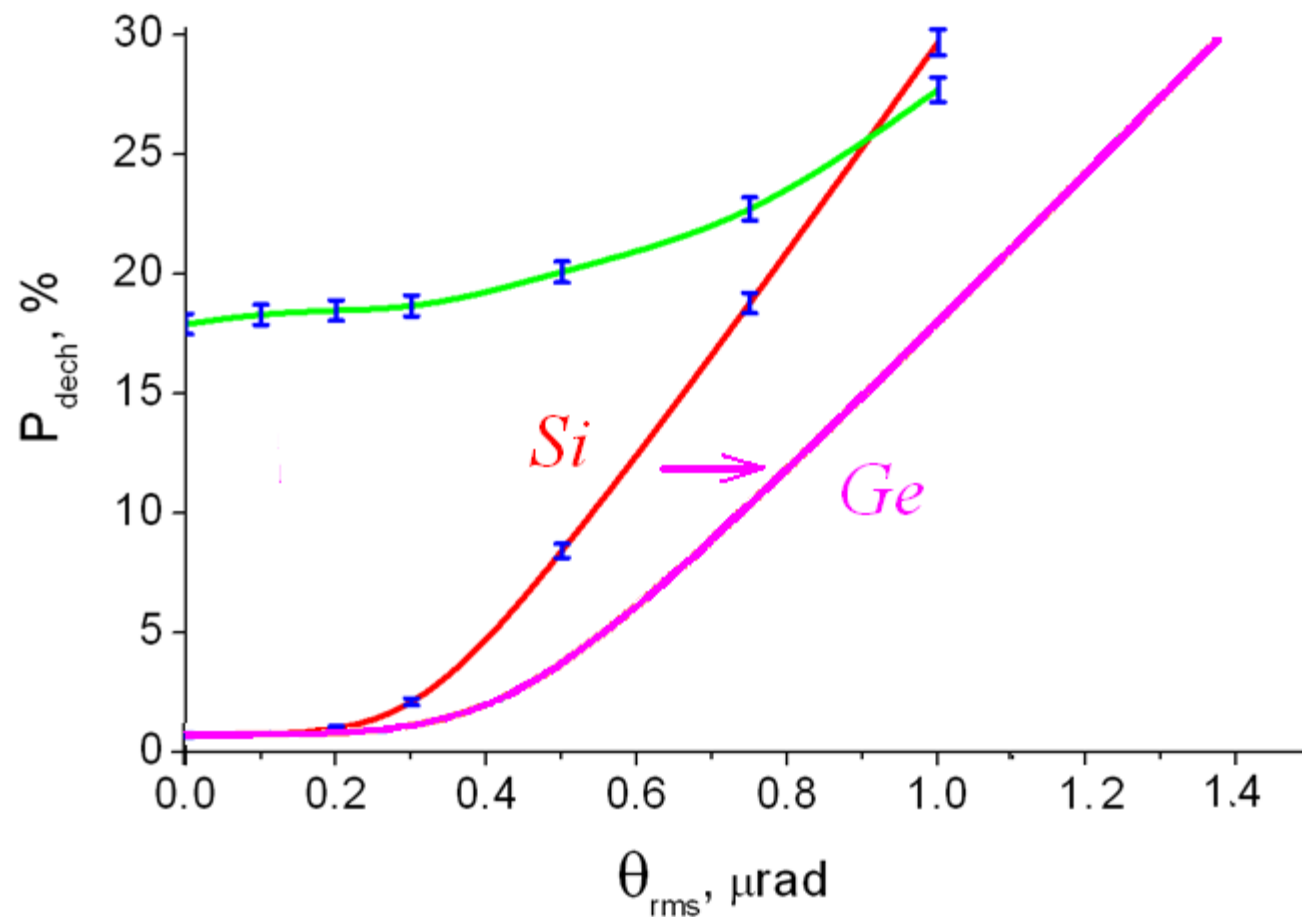
First MVROC observation

W. Scandale et al, PLB 682(2009)274



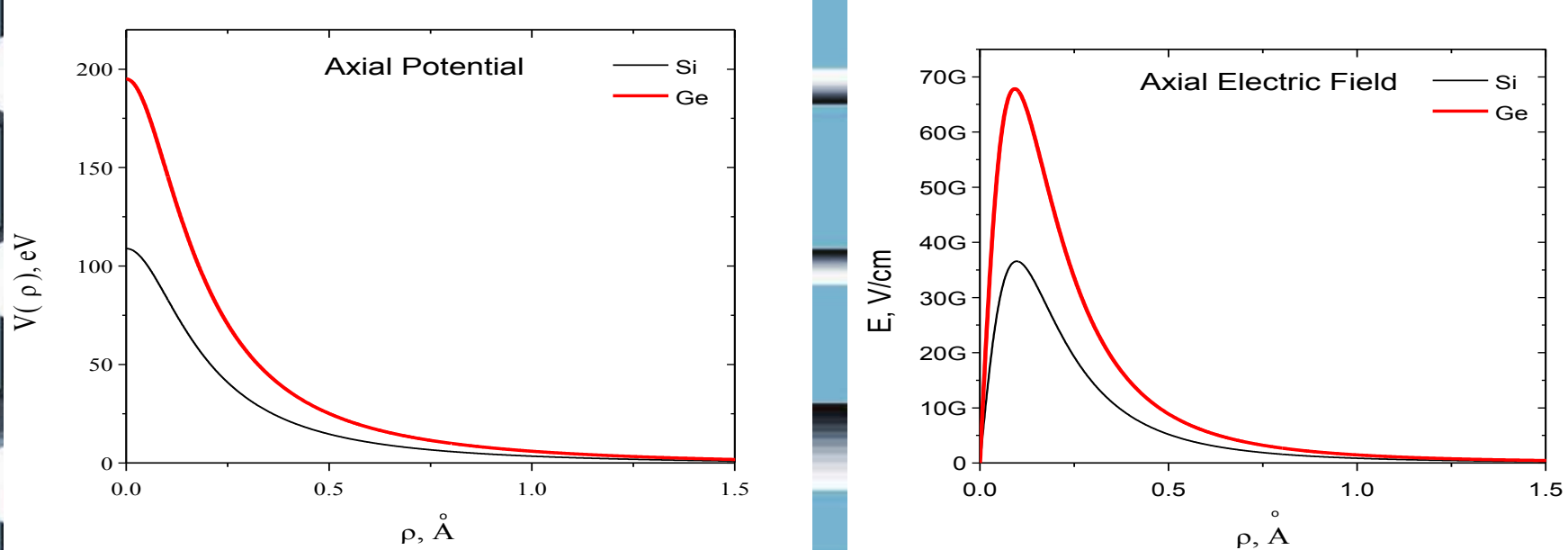
MVROC indeed increases reflection angle **5 times**

Improvement of the cut action in Ge



Ge widens the cut acceptance by 40%

Comparison of axial potential and field strength in Si and Ge



Both potential and field strength are nearly **twice as large** in Si than in Ge

Comparison averaged potentials and field strengths of Ge and Si planes and axes

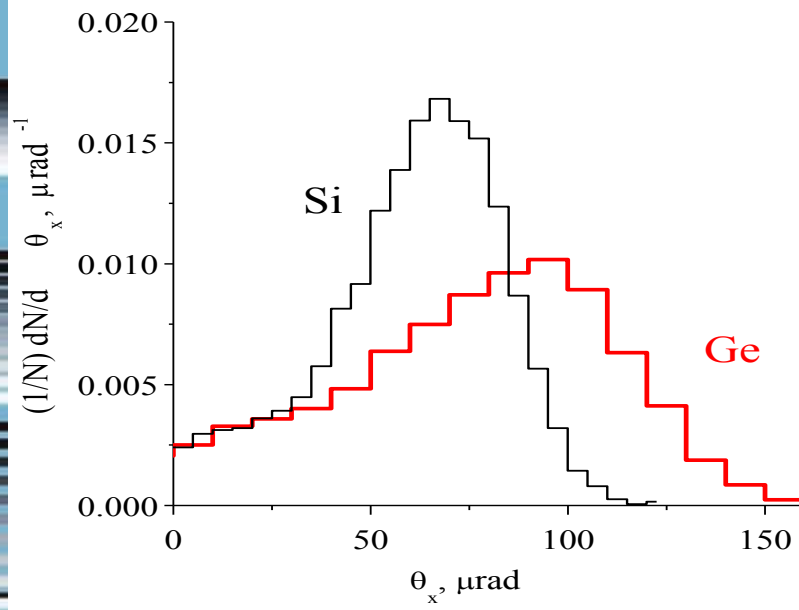
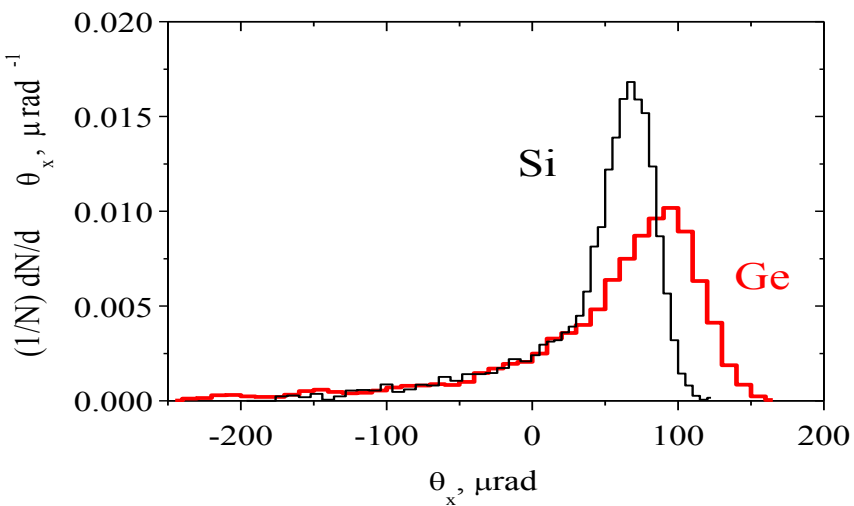
		Si(293K)	Ge(293K)	Ge(100K)	
<110>	V ₀ , eV	133	229	172%	309
<110>	E _{max} , GV/cm	46	78	170%	144
		Si(293K)	Ge(293K)	Ge(0K)	
(110)	V ₀ , eV	21.5	37.7	175%	44.0
(110)	E _{max} , GV/cm	5.7	9.9	1.74	14.9

u(293K)=0.085Å, u(100K)=0.054Å, u(0K)=0.036Å

Ge cooling is very productive!

Volume reflection angle increase in Ge

— Ge <111> 400 GeV 4mm 11.43/1.35m Vx=195*1.35 Vy=85*1.35
dvx=11, dvy=9.136 77.07/51.9
— Si <111> 400 GeV Gaussian asymmetric, $\delta\theta_x = 11\mu\text{rad}$, $\delta\theta_y = 9.13\mu\text{rad}$,
 $\theta_x = 195\mu\text{rad}$, $\theta_y = 85\mu\text{rad}$



Investigating Strong Field QED effects

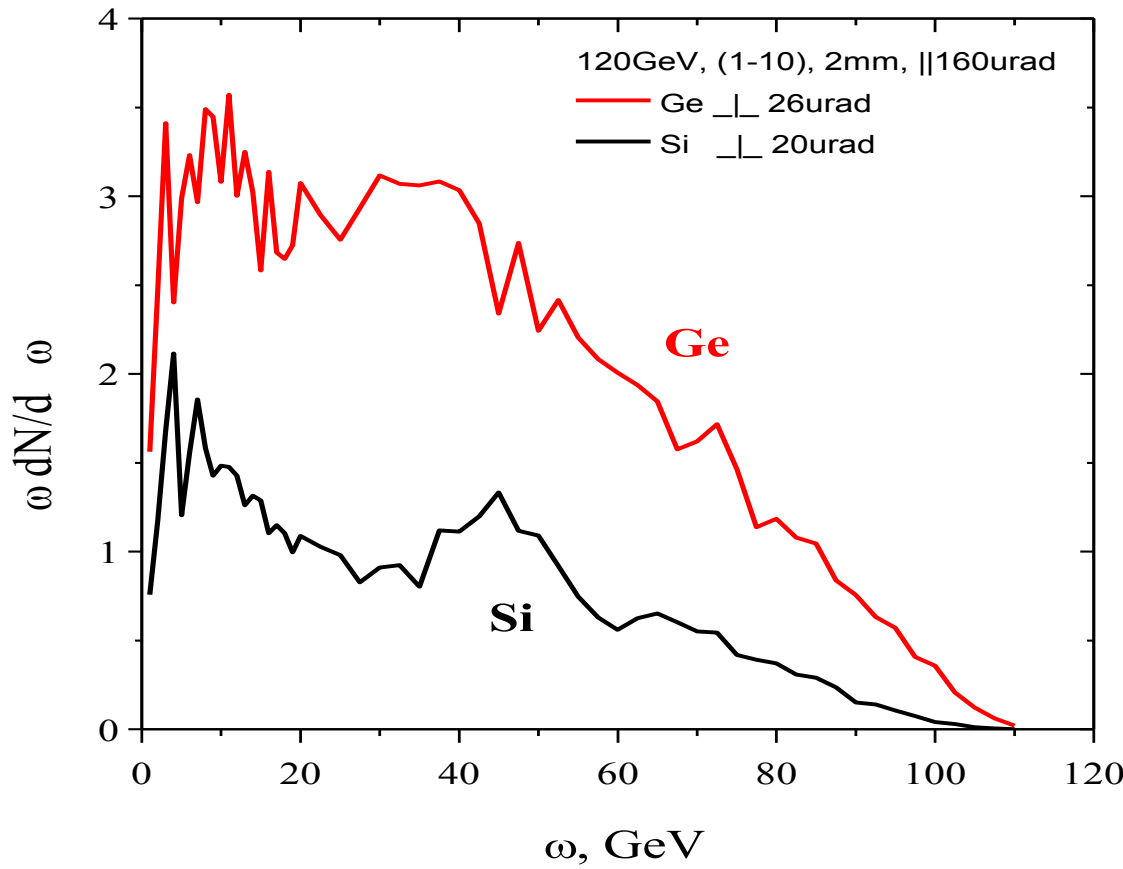
$$\chi = \frac{E}{1.32 \cdot 10^{16} eV/cm} \frac{\epsilon}{mc^2} \quad - \text{the main parameter of quantum electrodynamics}$$

		Si(293K)	Ge(293K)	Ge(100K)		
<110>	E _{max} , GV/cm	46	78	170%	144	313%
	χ(120GeV)	0.82	1.39		2.56	

$$I(\chi \ll 1) \propto E^2,$$
$$I(\chi \sim 1) \propto E,$$
$$I(\chi \gg 1) \propto E^{2/3}$$

Radiation intensity will grow like $E \div E^2$

Increase of radiated photon number in Germanium



The increase exceeds two